New Nickel−Antimony Carbonyl Clusters: Stereochemical Analyses of the $[Ni_{10}(SbR)_2(CO)_{18}]^{2-}$ Dianions (R = Me, Et, ^{i}Pr, ^{t}Bu, *p*-FC_6H_4) Containing Empty 1,12-$Ni_{10}Sb_2$ Icosahedral Cages and of the Unprecedented Stibinido-Bridged 34-Electron $Ni_2(CO)_4(\mu_2\text{-}Sb^tBu_2)_2$ Dimer[1]

Peter D. Mlynek and Lawrence F. Dahl*

Department of Chemistry, University of Wisconsin−Madison, Madison, Wisconsin 53706

Received November 15, 1996[⊗]

Reactions of $[Ni_6(CO)_{12}]^{2-}$ (**1**) with R_2SbBr (R = Me, Et, ^{i}Pr) and R_2SbCl (R = ^{t}Bu, *p*-FC_6H_4) have given rise to the new $[Ni_{10}(SbR)_2(CO)_{18}]^{2-}$ complexes (R = Me (**3**), Et (**4**), ^{i}Pr (**5**), ^{t}Bu (**6**), *p*-FC_6H_4 (**7**)) as the only major Ni−Sb product in each reaction (30−55% yields isolated as $[NMe_4]^+$ salts). These dianions, each of which has a crystallographically imposed inversion center, possess a common noncentered 1,12-$Ni_{10}Sb_2$ icosahedral cage that is surrounded by a 20-vertex ligand polyhedron composed of 10 terminal, 4 doubly bridging, and 4 triply bridging COs and the two Sb-attached R substituents. The formulation of each dianion was unambiguously established from X-ray crystallographic and infrared studies. An elemental analysis of $[NMe_4]_2$[**3**] substantiated its stoichiometry; magnetic susceptibility measurements conclusively showed this salt to be diamagnetic at room temperature. Cyclic voltammetric measurements of **3** and **5** in acetonitrile solutions similarly displayed only irreversible oxidation waves at *ca.* +0.60 V. A negative-ion electrospray ionization (ESI) mass spectrum of $[NMe_4]_2$[**5**] revealed the doubly charged ion-parent (M^{2-}) signal for the dianion (**5**) as well as 11 other assigned doubly charged high-range *m*/*z* signals. In light of the previously known phenylstibinidene $[Ni_{10}(SbPh)_2(CO)_{18}]^{2-}$ (**2**) prepared from reactions of **1** with either $PhSbCl_2$ or Ph_2SbCl, reactions of **1** with PhMeSbX (X = Br, I) were carried out; only **3** was isolated. Limiting slow-exchange $^{13}C\{^1H\}$ spectra were obtained at −60 °C for both **3** and **5** in acetone-d_6; a variable-temperature line-shape analysis of the terminal-bridge carbonyl exchange process in **5** gave an estimated activation energy of 52.5 kJ/mol. One achieved objective was to assess the resulting steric effects due to a systematic change of the Sb-attached R substituents upon both the geometries of the common empty 1,12-$Ni_{10}Sb_2$ cage and the encapsulating 20-vertex ligand polyhedron. Another goal was to determine the possible existence for E = Sb of the other two hypothetical $[Ni_9(ER)_3(CO)_{15}]^{2-}$ and $[Ni_8(ER)_4(CO)_{12}]^{2-}$ dianions containing empty 1,2,12-Ni_9E_3 and 1,2,9,12-Ni_8E_4 icosahedral cages, respectively; previous work had shown the existence of all three electronically equivalent (isolobal) dianions for E = P and As but only **2** for E = Sb with R = Ph. Despite extensive efforts to detect such species, no evidence for their existence was uncovered. However, a neutral 34-electron $Ni_2(CO)_4(\mu_2\text{-}Sb^tBu_2)_2$ dimer (**8**) containing a planar Ni_2Sb_2 core was isolated as a side product and structurally characterized; this dimer is the first example of a stibinido-bridged analogue of the known 34-electron $Ni_2(CO)_4(\mu_2\text{-}PR_2)_2$-type dimer. A structural/bonding analysis with other 34-, 32-, and 30-electron $Ni_2(\mu_2\text{-}ER_2)_2$ dimers (E = P, As) containing analogous planar Ni_2E_2 rings provides a self-consistent basis that a strong Ni−Ni′ bonding interaction between two Ni(I) plays a dominant role in dictating the observed geometry of each of these ligand-bridged dimers. This comparison also indicates that an essential ingredient for the existence of **8** as a stable entity is the bulky Sb-attached ^{t}Bu substituents which apparently protect the dimer from air oxidation.

Introduction

During the last 35 years both noncentered (empty) and centered (filled) icosahedra, a polyhedron that *per se* has 12 vertices, 20 triangular faces, and 30 edges, have been widely represented as a prominent geometrical unit in primarily main-group clusters, especially those containing boron. The existence of the icosahedron as a regular discrete noncentered deltahedron (*i.e.*, a *closo* triangulated polyhedron) of I_h symmetry, corresponding to one of the five Plato solids[2] with identical vertices and with all faces alike, was first

* To whom correspondence should be addressed. E-mail: dahl@chem.wisc.edu. Fax: +608-262-0381.

⊗ Abstract published in *Advance ACS Abstracts,* March 15, 1997.

(1) (a) Presented in part at the 208th National Meeting of the American Chemical Society, Washington, DC, Aug 24, 1994. See: Mlynek, P. D.; Dahl, L. F., *Abstracts of Papers;* 208th National Meeting of the American Chemical Society; American Chemical Society: Washington, DC, 1994; INOR 561. (b) Based in part on the Ph.D. thesis of P.D.M. at the University of Wisconsin−Madison, 1996.

S0276-7333(96)00966-1 CCC: $14.00

exemplified by the classic $[B_{12}H_{12}]^{2-}$ dianion from both theoretical and experimental analyses.[3,4] Clusters containing noncentered icosahedral frameworks were also found for a wide range of carboranes, such as 1,2-$C_2B_{10}H_{12}$, 1,7-$C_2B_{10}H_{12}$, and 1,12-$C_2B_{10}H_{12}$, and metallocarboranes, in which a skeletally substituted carborane was shown to contain one, two, or three metal atoms.[5,6] Distorted noncentered icosahedral geometries for a number of other discrete noncentered main group-borane clusters are now known including 1,2-$E_2B_{10}H_{10}$ (E = P,[7] As,[8] Sb,[9] Bi[10]). Recent work also includes the preparation of $[Al_{12}R_{12}]^{2-}$ (R = ^{i}Bu),[11] a group III (13) analogue of $[B_{12}H_{12}]^{2-}$, that likewise has a regular noncentered icosahedral geometry and possesses $n + 1 = 13$ skeletal electron pairs in accordance with electron-counting rules for an *n*-vertex deltahedron.[12]

The centered icosahedron has been an important basic building block observed in extended icosahedral materials, such as several allotropes of boron,[13] complex borides,[13,14] gallides,[15,16] and quasi-crystalline aluminum alloys.[16−18] Centered icosahedra have also been formulated as structural entities in amorphous materials[19] and in the growth of small metal particles.[20] Furthermore, theoretical calculations have indicated for normally face-centered cubic materials such as nickel metal that the minimum energy-packing geometry is the 13-atom centered icosahedron.[21] Initial crystallographically characterized examples of discrete non-boron-containing clusters with centered icosahedral cages are the $[Rh_{12}Sb(CO)_{27}]^{3-}$ with a Sb-centered Rh_{12} icosahedral cage[22] and the $[Au_{13}(PPhMe_2)_{10}Cl_2]^{3+}$ with a Au-centered Au_{12} icosahedral cage.[23] Comprehensive investigations by Teo, Zhang, and co-workers[24,25] in this area have given rise to a remarkable series of bimetallic Au/Ag "supraclusters" whose metal frameworks are described in terms of polyicosahedra based upon the vertex-sharing of 13-atom Au-centered icosahedra. More recently, trimetallic Au/Ag/Ni and Au/Ag/Pt polyicosahedral supraclusters were also reported.[26]

In sharp contrast, up to 12 years ago, the conformity of transition metal carbonyl clusters to icosahedral geometries was uncommon, the only example having been the Sb-centered $[Rh_{12}Sb(CO)_{27}]^{3-}$ trianion.[22] However, during the last decade there has been a marked surge of experimental−theoretical studies in transition-metal cluster chemistry involving the icosahedron; preparative work from our laboratories[27−34] and from those of Longoni and co-workers[35−38] has resulted in a wide variety of different main-group atoms being incorporated along with nickel atoms into both noncentered and centered icosahedra.

(2) (a) Hargittai, I.; Hargittai, M. *Symmetry through the Eyes of a Chemist*, 2nd ed.; Plenum Press: New York, 1995; pp 79−81. (b) Hargittai, I.; Hargittai, M. *Symmetry: A Unifying Concept*; Shelter Publications: Bolinas, CA, 1994; pp 90−91. (c) Wells, A. F. *Structural Inorganic Chemistry*, 5th ed.; Oxford University Press: London, 1984; pp 69−71.

(3) (a) Lipscomb, W. N.; Wunderlich, J. A. *J. Am. Chem. Soc.* **1960**, *82*, 4427−4428. (b) Pitochelli, A. R.; Hawthorne, M. F. *J. Am. Chem. Soc.* **1960**, *82*, 3228−3229. (c) Muetterties, E. L.; Merrifield, R. E.; Miller, H. C.; Knoth, W. H., Jr.; Downing, J. R. *J. Am. Chem. Soc.* **1962**, *84*, 2506−2508.

(4) (a) Longuet-Higgens, H. C.; Roberts, M. de V. *Proc. R. Soc. (London), Ser. A* **1955**, *230*, 110−119. (b) Hoffmann, R.; Lipscomb, W. N. *J. Chem. Phys.* **1962**, *36*, 2179−2189.

(5) See, for example: (a) Muetterties, E. L.; Knoth, W. H. *Polyhedral Boranes*; Marcel Dekker: New York, 1968; pp 21−31. (b) Cotton, F. A.; Wilkinson, G. *Advanced Inorganic Chemistry*, 5th ed.; John Wiley & Sons: New York, 1988; pp 162−207 and references therein.

(6) (a) Grimes, R. N. *Carboranes*; Academic Press: New York, 1970. (b) Greenwood, N. N.; Earnshaw, A. *Chemistry of the Elements*; Pergamon Press: New York, 1984; pp 206−213. (c) Grimes, R. N. In *Comprehensive Organometallic Chemistry*; Wilkinson, G., Stone, F. G. A., Abel, E. W., Eds.; Pergamon Press: New York, 1984; Vol. I, pp 459−542. (d) Ferguson, G.; Hawthorne, M. F.; Kaitner, B.; Lalor, F. J. *Acta Crystallogr., Sect. C* **1984**, *C40*, 1707−1709. (e) O'Neill, M. E.; Wade, K. In *Metal Interactions with Boron Clusters*; Grimes, R. N., Ed.; Plenum Press: New York, 1982; pp 1−36.

(7) Little, J. L.; Kester, J. G.; Huffman, J. C.; Todd, L. J. *Inorg. Chem.* **1989**, *28*, 1087−1091.

(8) Hanusa, T. P.; Roig de Parisi, N.; Kester, J. G.; Arafat, A.; Todd, L. J. *Inorg. Chem.* **1987**, *26*, 4100−4102.

(9) Little, J. L. *Inorg. Chem.* **1979**, *18*, 1598−1600.

(10) Little, J. L.; Whitesell, M. A.; Kester, J. G.; Folting, D.; Todd, L. J. *Inorg. Chem.* **1990**, *29*, 804−808.

(11) Hiller, W.; Klinkhammer, K.-W.; Uhl, W.; Wagner, J. *Angew. Chem., Int. Ed. Engl.* **1991**, *30*, 179−180.

(12) (a) Wade, K. *J. Chem. Soc., Chem. Commun.* **1971**, 792−793. (b) Wade, K. *Electron Deficient Compounds;* Thomas Nelson and Sons: London, 1971. (c) Wade, K. *Adv. Inorg. Chem. Radiochem.* **1976**, *18*, 1−66.

(13) Hoard, J. L.; Hughes, R. E. *The Chemistry of Boron and its Compounds;* Muetterties, E. L., Ed.; J. Wiley & Sons: New York, 1967; Chapter 2, pp 25−154.

(14) Burdett, J. K.; Canadell, E. *J. Am. Chem. Soc.* **1990**, *112*, 7207−7217.

(15) Belin, C. *Acta Crystallogr., Sect. B* **1981**, *37*, 2060−2062.

(16) (a) Schäfer, H. *J. Solid-State Chem.* **1985**, *57*, 97−111. (b) Belin, C.; Ling, R. G. *J. Solid-State Chem.* **1983**, *48*, 40−48. (c) Belin, C.; Charbonnel, M. *J. Solid-State Chem.* **1986**, *64*, 57−66. (d) Charbonnel, M.; Belin, C. *J. Solid-State Chem.* **1987**, *67*, 210−218. (e) King, R. B. *Inorg. Chem.* **1989**, *28*, 2796−2799.

(17) (a) King, R. B. *Inorg. Chim. Acta* **1991**, *181*, 217−225 and references therein. (b) King, R. B. *Inorg. Chim. Acta* **1992**, *198*−200, 841−861 and references therein.

(18) *Extended Icosahedral Structures: Aperiodicity and Order*; Jarić, M. V., Gratias, D., Eds.; Academic Press: New York, 1989; Vol. 3, pp 1−219.

(19) (a) Machizaud, F.; Kuhnast, F. A.; Flechon, J. *Ann. Chim. (Paris)* **1978**, *3*, 177−186. (b) Briant, C. L.; Burton, J. J. *Phys. Status Solidi B* **1978**, *85*, 393−402.

(20) Renou, A.; Gillet, M. *Surf. Sci.* **1981**, *106*, 27−34 and references cited therein.

(21) (a) Rösch, N.; Knappe, P.; Sandle, P.; Gorling, A.; Dunlap, B. I. In *The Challange of d and f Electrons*; Salahub, D. R., Zerner, M. C., Eds.; American Chemical Society Symposium Series 394; American Chemical Society: Washington, DC, 1989. (b) Knickelbein, M. B.; Yang, S.; Riley, S. J. *J. Chem. Phys.* **1990**, *93*, 94−104. (c) Parks, E. K.; Zhu, L.; Ho, J.; Riley, S. J. *J. Chem. Phys.* **1994**, *100*, 7206−7222. (d) Estiú, G. L.; Zerner, M. C. *J. Phys. Chem.* **1994**, *98*, 9972−9978.

(22) Vidal, J. L.; Troup, J. M. *J. Organomet. Chem.* **1981**, *213*, 351−363.

(23) (a) Briant, C. E.; Theobald, B. R. C.; White, J. W.; Bell, L. K.; Mingos, D. M. P.; Welch, A. J. *J. Chem. Soc., Chem. Commun.* **1981**, 201−202. (b) Mingos, D. M. P. *Philos. Trans. R. Soc. London, A* **1982**, *No. 308*, 75−83.

(24) Teo, B. K.; Zhang, H. *Proc. Natl. Acad. Sci. U.S.A.* **1991**, *88*, 5067−5071 and references therein.

(25) Teo, B. K.; Zhang, H.; Kean, Y.; Dang, H.; Shi, X. *J. Chem. Phys.* **1993**, *99*, 2929−2941 and references therein.

(26) (a) Teo, B. K.; Zhang, H.; Shi, X. *J. Am. Chem. Soc.* **1993**, *115*, 8489−8490. (b) Teo, B. K.; Zhang, H.; Shi, X. *Inorg. Chem.* **1994**, *33*, 4086−4097. (c) Teo, B. K.; Zhang, H. *Coord. Chem. Rev.* **1995**, *143*, 611−636.

(27) Rieck, D. F.; Rae, A. D.; Dahl, L. F. *Abstracts of Papers;* 190th National Meeting of the American Chemical Society, Chicago, IL, Sept 1985; American Chemical Society: Washington, DC, 1985; INOR 157.

(28) Rieck, D. F.; Montag, R. A.; McKechnie, T. S.; Dahl, L. F. *J. Am. Chem. Soc.* **1986**, *108*, 1330−1331.

(29) DesEnfants, R. E., II; Gavney, J. A., Jr.; Hayashi, R. K.; Rae, A. D.; Dahl, L. F.; Bjarnason, A. *J. Organomet. Chem.* **1990**, *383*, 543−572.

(30) Rieck, D. F.; Gavney, J. A., Jr.; Norman, R. L.; Hayashi, R. K.; Dahl, L. F. *J. Am. Chem. Soc.* **1992**, *114*, 10369−10379.

(31) Zebrowski, J. P.; Hayashi, R. K.; Bjarnason, A.; Dahl, L. F. *J. Am. Chem. Soc.* **1992**, *114*, 3121−3123.

(32) Kahaian, A. J.; Thoden, J. B.; Dahl, L. F. *J. Chem. Soc., Chem. Commun.* **1992**, 353−355.

(33) Zebrowski, J. P.; Hayashi, R. K.; Dahl, L. F. *J. Am. Chem. Soc.* **1993**, *115*, 1142−1144.

(34) Mlynek, P. D.; Dahl, L. F. *Organometallics*, **1997**, *16*, 1655.

(35) Ceriotti, A.; Demartin, F.; Heaton, B. T.; Ingallina, P.; Longoni, G.; Manassero, M.; Marchionna, M.; Masciocchi, N. *J. Chem. Soc., Chem. Commun.* **1989**, 786−787.

(36) Albano, V. G.; Demartin, F.; Iapalucci, M. C.; Longoni, G.; Sironi, A.; Zanotti, V. *J. Chem. Soc., Chem. Commun.* **1990**, 547−548.

(37) Albano, V. G.; Demartin, F.; Iapalucci, M. C.; Laschi, F.; Longoni, G.; Sironi, A.; Zanello, P. *J. Chem. Soc., Dalton Trans.* **1991**, 739−748.

(38) Albano, V. G.; Demartin, F.; Iapalucci, M. C.; Longoni, G.; Monari, M.; Zanello, P. *J. Chem. Soc., Dalton Trans.* **1992**, 497−502.

Our first crystallographically characterized examples of such clusters with a noncentered icosahedral cage were the nickel−methylarsinidene $[Ni_{10}(AsMe)_2(CO)_{18}]^{2-}$ dianion with a 1,12-$Ni_{10}As_2$ cage and the nickel-phenylarsinidene $[Ni_9(AsPh)_3(CO)_{15}]^{2-}$ dianion with a 1,2,12-Ni_9As_3 cage;[27,28] these were isolated from reactions of $[Ni_6(CO)_{12}]^{2-}$ dianion (**1**)[39] with $MeAsBr_2$ and $PhAsCl_2$, respectively. These investigations led to the preparation and stereochemical characterization of the structurally analogous nickel−phosphinidene $[Ni_{10}(PMe)_2(CO)_{18}]^{2-}$ and $[Ni_9(PMe)_3(CO)_{15}]^{2-}$ dianions[30] by reactions of **1** with $MePCl_2$.

Parallel work in our laboratories involving reactions of **1** with either diphenylantimony chloride, Ph_2SbCl, or phenylantimony dichloride, $PhSbCl_2$, in THF solutions at room temperature gave as the main product (50−60% yields) only $[Ni_{10}(SbPh)_2(CO)_{18}]^{2-}$ (**2**); its identity was unambiguously established from X-ray diffraction determinations of this dianion in four different crystalline compounds—*viz.*, THF- and acetone-solvated $[NMe_4]^+$, THF-solvated $[(PPh_3)_2N]^+$, and $[NMe_3Ph]^+$ salts.[29] A comparative analysis revealed that the dianion (**2**) in each of these ionic salts possesses a virtually identical geometry consisting of a 1,12-disubstituted $Ni_{10}Sb_2$ icosahedral cage of crystallographic C_i-$\bar{1}$ site symmetry encapsulated by two antimony-attached phenyl substituents and 10 terminal, 4 doubly bridging, and 4 triply bridging COs. The fact that **2** was the only nickel−stibinidene carbonyl cluster isolated from the room-temperature reaction with the Ph_2SbCl reactant was attributed to the facile cleavage of one of the two Sb−Ph bonds of the Ph_2SbCl under the reaction conditions as well as to the apparent thermodynamic stability of **2**. The utilization of different counterions and reaction conditions was a consequence of attempts to determine whether the hypothetical phenylstibinidene Ni_9Sb_3 analogue of the known $[Ni_9(ER)_3(CO)_{15}]^{2-}$ dianions (E = P, R = Me,[27,30] E = As, R = Ph[28]) existed; however, no spectral or crystallographic evidence was found for its existence. Each of the noncentered icosahedral clusters is electronically equivalent to the regular noncentered $[B_{12}H_{12}]^{2-}$ icosahedron in possessing 13 skeletal electron pairs.

Important complementary research by Longoni and co-workers involving reactions of **1** with main-group halide reagents has given rise to several new types of related clusters—*viz.*, $[Ni_{12}E(CO)_{22}]^{2-}$ dianions (E = Sn, Ge) with E-centered Ni_{12} icosahedral cages,[35] the $[Ni_{10}Ge(CO)_{20}]^{2-}$ dianion with a Ge-centered Ni_{10} pentagonal antiprismatic cage (*i.e.*, an icosahedron with two missing 1,12-vertices),[35] the $[Ni_{11}\{SbNi(CO)_3\}_2(CO)_{18}]^{n-}$ anions (n = 2, 3, 4) with Ni-centered 1,12-$Ni_{10}Sb_2$ icosahedral cages and Sb-attached $Ni(CO)_3$ substituents,[36,37] and the $[Ni_{11}Bi_2(CO)_{18}]^{n-}$ anions (n = 2, 3, 4) with Ni-centered 1,12-$Ni_{10}Bi_2$ icosahedral cages and no Bi-attached substituents.[38] Bonding analyses of these clusters were carried out in order to rationalize the unusual electron counts of the Ni-centered icosahedral clusters which did not conform to the 13 skeletal electron count observed in the related noncentered or main-group-centered icosahedral systems; it was concluded that the centered (interstitial) nickel atom can affect both the cluster electronic requirements and the ligand stereochemistry and therefore cannot merely be considered as an "innocent" internal ligand.[37,40]

In all of the above research, only solvent extractions and metathesis counterion reactions were utilized to separate the anionic products. In fact, samples of $[Ni_9(PMe)_3(CO)_{15}]^{2-}$ as the $[NMe_4]^+$ salt were invariably contaminated with $[NMe_4]^+_2[Ni_{10}(PMe)_2(CO)_{18}]^{2-}$ such that the pure Ni_9P_3 cluster was originally obtained in the Pasteur fashion by microscopic crystal separation.[27] The subsequent application in our laboratories of column chromatographic separation procedures involving the use of silica gel support under anaerobic conditions, initially developed for separation and identification of large anionic platinum carbonyl clusters,[41] for the isolation of anionic products from further reactions of **1** with $MePCl_2$ resulted in the clean separation not only of the 1,12-$Ni_{10}P_2$ and 1,2,12-Ni_9P_3 icosahedral clusters but also of three initially undetected clusters including $[Ni_8(PMe)_4(CO)_{12}]^{2-}$, which is the third member of the homologous $[Ni_{12-x}(PMe)_x(CO)_{24-3x}]^{2-}$ series (x = 2, 3, 4).[30] The three corresponding phenylphosphinidene members of the analogous $[Ni_{12-x}(PPh)_x(CO)_{24-3x}]^{2-}$ series (x = 2, 3, 4) have also been isolated via similar chromatographic separations.[42]

The fact that the above work showed that both the noncentered and centered icosahedron is a dominant polyhedron for nickel carbonyl clusters containing main-group V (15) atoms raised the question as to whether main-group IV (14) or VI (16) atoms could also be incorporated into icosahedral $Ni_{12-x}E_x$ frameworks. Reactions of **1** with main-group IV (14) reagents produced $[Ni_{11}(ER)_2(CO)_{18}]^{2-}$ dianions (E = Sn, R = Me, ^{n}Bu;[33] E = Ge, R = Et[31]) with Ni-centered 1,12-$Ni_{10}Sn_2$ and 1,12-$Ni_{10}Ge_2$ icosahedral cages. Likewise, reactions of **1** with main-group VI (16) reagents gave rise to $[Ni_{11}E_2(CO)_{18}]^{2-}$ (E = Se, Te), $[Ni_{10}Te_3(CO)_{15}]^{2-}$, and $[Ni_8Te_4(CO)_{12}]^{2-}$ with Ni-centered 1,12-$Ni_{10}E_2$, Ni-centered 1,2,12-Ni_9Te_3, and noncentered 1,2,9,12-Ni_8Te_4 icosahedral cages, respectively.[32] These new families of discrete icosahedral clusters provided structural/bonding analyses of geometrical effects related to the presence or absence of the internal Ni(*i*) atom, from which it was concluded[32,33] that current electron-counting rules[43] do not work in general when applied to icosahedral cage clusters containing interstitial (internal) Ni(*i*) atoms.

In a comprehensive analysis, Teo, Zhang, and co-workers[25] recently reported the systematic determination of all possible stereoisomers for both noncentered and centered binary icosahedra—*i.e.*, heteronuclear ones with two different kinds of atoms and homonuclear ones with either two different ligand environments or with missing vertices (holes). In addition, atom- and electron-counting rules were presented in order to account for the observed variations in electron counts in different binary icosahedral clusters.

(39) (a) Calabrese, J. C.; Dahl, L. F.; Cavalieri, A.; Chini, P.; Longoni, G.; Martinengo, S. *J. Am. Chem. Soc.* **1974**, *96*, 2616−2618. (b) Longoni, G.; Chini, P.; Cavalieri, A. *Inorg. Chem.* **1976**, *15*, 3025−3029.

(40) Sironi, A. *J. Chem. Soc., Dalton Trans.* **1993**, 173−178.

(41) Lewis, G. J.; Hayashi, R. K.; Dahl, L. F. *Abstracts of Papers* (*Part 1*); 3rd Chemical Congress of North America, Toronto, Canada, June 1988; American Chemical Society: Washington, DC, 1988; INOR 660.

(42) Bacon, J. W. Ph.D. Thesis, University of Wisconsin−Madison, 1994.

(43) Mingos, D. M. P.; Zhenyang, L. *J. Chem. Soc., Dalton Trans.* **1988**, 1657−1664 and references therein. (b) Mingos, D. M. P.; May, A. P. In *The Chemistry of Metal Cluster Complexes*; Shriver, D. F., Kaesz, H. D., Adams, R. D., Eds.; VCH Publishers: New York, 1990; Chapter 2, pp 11−119. (c) Mingos, D. M. P.; Wales, D. J. *Introduction to Cluster Chemistry*; Prentice Hall: Old Tappan, NJ, 1990.

The research presented herein has involved reactions of $[Ni_6(CO)_{12}]^{2-}$ (**1**)[39] with one aryl and several different alkyl antimony precursors and the characterization of resulting isolated products by X-ray crystallographic, spectroscopic, and electrochemical measurements. Envisioned major goals have included the following: (1) an examination of the effects of a systematic change of antimony-bound alkyl ligands on the cage structures as well as on the ligand polyhedra of the $[Ni_{10}(SbR)_2(CO)_{18}]^{2-}$ dianions; (2) the possible isolation of hypothetical Ni_9Sb_3 or Ni_8Sb_4 analogues of those in the homologous $[Ni_{12-x}(PMe)_x(CO)_{24-3x}]^{2-}$ series ($x = 2, 3, 4$);[30] (3) an examination of variable-temperature ^{13}C NMR spectra of an 1,12-$Ni_{10}Sb_2$ cluster to determine the possible existence and nature of fluxional carbonyl behavior between the terminal and bridging carbonyl ligands; (4) cyclic voltammetric measurements of these clusters in order to determine whether reversible electron transfer occurs in these 13 electron-pair systems. The results presented here have fulfilled our objectives. In addition, an unprecedented 34-electron $Ni_2(CO)_4(\mu_2\text{-}Sb^tBu_2)_2$ dimer was isolated as a side product and structurally characterized; a comparative geometrical analysis with other related 34-, 32-, and 30-electron $Ni_2(\mu_2\text{-}ER_2)_2$ dimers (E = P, As)[44−51] has evolved into an integrated bonding description that strong Ni−Ni′ bonding interactions between two Ni(I) atoms are responsible for producing similar deformations in the planar Ni_2E_2 rings of these dimers.

Results and Discussion

Syntheses of Dialkylantimony Monohalide Reagents. Due to the different physical properties of the intermediates, variations in the synthetic routes to obtain dialkylantimony monohalides were used. The synthesis of dimethylantimony bromide[52,53] was achieved by initial formation of trimethylantimony from a Grignard reaction of antimony trichloride with 3 equiv of methylmagnesium iodide; subsequent bromination gave rise to Me_3SbBr_2, which upon being heated decomposed to methyl bromide and the desired Me_2SbBr. This method was modified for obtaining the corresponding ethyl and isopropyl R_2SbBr analogs in that the intermediate R_3Sb was not isolated; the formed dialkylantimony bromide was instead isolated by fractional distillation. An alternative preparative route for the formation of di-*tert*-butylantimony bromide was carried out, because tri-*tert*-butylantimony does not undergo bromination readily due to the steric crowding around the antimony center by the bulky *tert*-butyl groups.[54] Consequently, di-*tert*-butylantimony chloride was formed by reaction of two equiv of *tert*-butylmagnesium bromide with antimony trichloride; in contrast to the other dialkyl halides, this product was not obtained in high purity. Slight overbutylation or slight underbutylation of the antimony precursor resulted in contamination of the desired product by tri-*tert*-butylantimony and *tert*-butylantimony dichloride, respectively.

Metathesis can also be used for the formation of any of the R_2SbX reagents synthesized above, simply by reaction of the intermediate trialkylantimony with antimony trihalide in a 2:1 ratio at appropriate conditions;[55,56] this procedure was used to form $MeSbCl_2$. By reversing this molar ratio of trialkylantimony to antimony trihalides, we were successful in obtaining alkylantimony dihalides, such as methylantimony dichloride and methylantimony dibromide. Metathesis was also used to obtain phenylantimony dibromide from commercially available triphenylantimony and antimony tribromide; further reaction of phenylantimony dibromide with a $^1/_3$ equiv of methylmagnesium iodide gave the desired phenylmethylantimony bromide.

Syntheses of $[Ni_{10}(SbR)_2(CO)_{18}]^{2-}$ Dianions (R = Me (3), Et (4), ^{i}Pr (5), ^{t}Bu (6), *p*-FC_6H_4 (7)). Although there are major significant differences between the reactions of the $[Ni_6(CO)_{12}]^{2-}$ dianion (**1**) with dihalophosphine and dihaloarsine reagents in obtaining different types of high-nuclearity nickel-group V (15) clusters, a variety of products was not observed in corresponding nickel−antimony reactions. Despite our search to synthesize and isolate large nickel−stibinidene clusters by use of halodialkylstibine reagents (instead of the previously utilized Ph_2SbCl and $PhSbCl_2$) under various reaction conditions, the $[Ni_{10}(SbR)_2(CO)_{18}]^{2-}$ dianion was the sole high-nuclearity product that was isolated. For example, only this $[Ni_{10}(SbMe)_2(CO)_{18}]^{2-}$ dianion (**3**)[57,58] was obtained when the syntheses were carried out with halodimethylstibine reagents in different high-polarity solvents such as acetone, THF, or acetonitrile. The reaction temperatures in forming this cluster were varied from −78 °C to slightly above room temperature; above 30 °C the reaction mixture gave an insoluble black powder. Reaction times, on the order of hours, were also not crucial; however, none of the clusters presented herein is sufficiently robust to last for days in the reaction mixture. **3** was obtained not only from reactions of **1** with dialkylantimony monohalides (*e.g.*, Me_2SbBr or Me_2SbCl) but also from reactions with dihaloalkylstibine reagents (*e.g.*, $MeSbCl_2$ or $MeSbBr_2$) under similar

(44) Jarvis, J. A. J.; Mais, R. H. B.; Owston, P. G.; Thompson, D. T. *J. Chem. Soc. A* **1970**, 1867−1872.
(45) Arif, A. M.; Jones, R. A.; Schwab, S. T. *J. Coord. Chem.* **1987**, *16*, 51−57.
(46) Jones, R. A.; Norman, N. C.; Seeberger, M. H.; Atwood, J. L.; Hunter, W. E. *Organometallics* **1983**, *2*, 1629−1634.
(47) Jones, R. A.; Stuart, A. L.; Atwood, J. L.; Hunter, W. E. *Organometallics* **1983**, *2*, 874−878.
(48) Deppisch, B.; Schäfer, H. *Z. Anorg. Allg. Chem.* **1982**, *490*, 129−135.
(49) Jones, R. A.; Stuart, A. L.; Atwood, J. L.; Hunter, W. E.; Rogers, R. D. *Organometallics* **1982**, *1*, 1721−1723.
(50) Barnett, B. L.; Krüger, C. *Cryst. Struct. Commun.* **1973**, *2*, 85−88.
(51) Jones, R. A.; Whittlesey, B. R. *Inorg. Chem.* **1986**, *25*, 852−856.
(52) Bromodimethylstibene, $SbMeBr_2$. We have also chosen to utilize the Gmelin nomenclature[53] throughout this paper in order not to confuse halide substitution on an organic ligand with a halogen σ-bonded directly to the antimony. We do not mean to convey an ionic relationship by this usage.
(53) Wieber, M. *Organoantimony Compounds, Part 2: Compounds of Trivalent Antimony with Two and One Sb−C Bonds*; Bitterer H., Ed.; Gmelin Handbook of Inorganic Chemistry, 8th ed.; Springer-Verlag: Berlin, 1981.
(54) Hartmann, H.; Kühl, G. *Z. Anorg. Allg. Chem.* **1961**, *312*, 186−194.
(55) Wieber, M.; Wirth, D.; Fetzer, I. *Z. Anorg. Allg. Chem.* **1983**, *505*, 134−137.
(56) Nunn, M.; Sowerby, D. B.; Wesolek, D. M. *J. Organomet. Chem.* **1983**, *251*, C45−C46.
(57) The designation of the cluster atoms was chosen to be consistent with similar compounds[29,30] for comparison purposes, instead of the strictly adhering to the IUPAC system which would number the nickel atoms differently. The systematic name[58] for $[NMe_4]_2$[**3**] is bis(tetramethylammonium) tetra-μ_3-carbonyl-2:3:7κ^3C;2:7:11κ^3C;4:5:9κ^3C;5:9:10κ^3C-tetra-μ-carbonyl-3:8κ^2C;4:8κ^2C;6:10κ^2C;6:11κ^2C-decacarbonyl-2κC,3κC,4κC,5κC,6κC,7κC,8κC,9κC,10κC,11κC-dimethyl-1κC,12κC-[I_h-(1551)-Δ^{20}-*closo*]1,12-diantimonidedecanickelate(20 *Ni*−*Ni*)(20 *Ni*−*Sb*)(2−).
(58) See, for example Section I-10.8.3. in: *Nomenclature of Inorganic Chemistry: Recommendations 1990*; Leigh, G. J., Ed.; Blackwell Scientific Publications: Oxford, U.K., 1990.

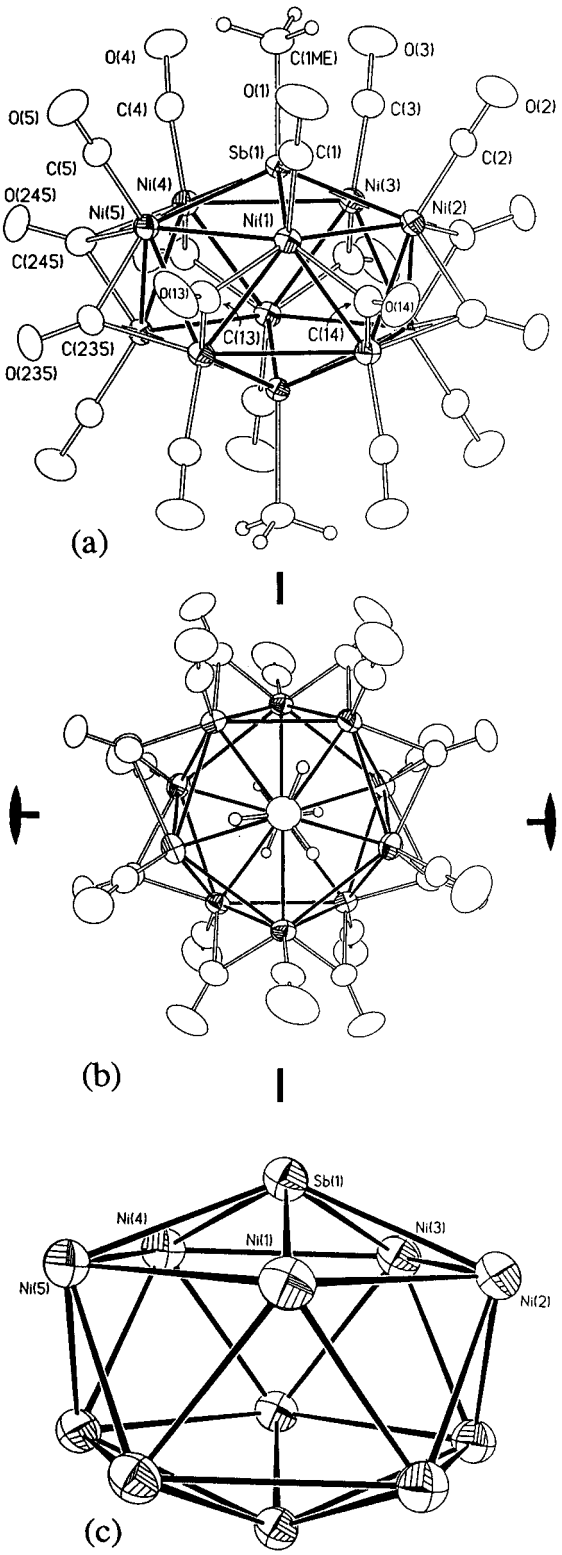

Figure 1. (a) Configuration of the $[Ni_{10}(SbMe)_2(CO)_{18}]^{2-}$ dianion (**3**) of crystallographic C_i-$\bar{1}$ site symmetry in the $[NMe_4]^+$ salt. The independent non-hydrogen atoms are labeled. (b) View of **2** along the idealized 5-fold Sb···Sb′ axis of the oblate 1,12-$Ni_{10}Sb_2$ icosahedral cage. Upon inclusion of the four doubly and four triply bridging carbonyl ligands, the pseudo-D_{5d} symmetry of the cage is reduced to pseudo C_{2h}-2/*m*; the resulting 2-fold axis and horizontal mirror plane are designated. (c) View of the noncentered 1,12-$Ni_{10}Sb_2$ icosahedral cage of **3**, which may be envisioned as a pentagonal antiprism of 10 surface Ni(*s*) atoms that is capped on both pentagonal faces by antimony atoms.

conditions. In order for the antimony reagent to produce **3** by reaction with **1**, it became apparent that the

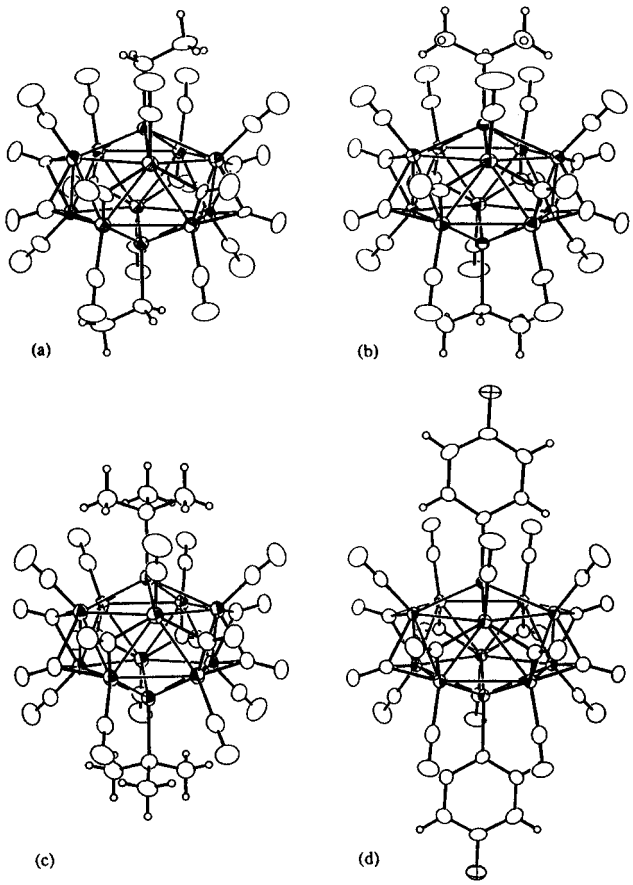

Figure 2. Configuration in the $[NMe_4]^+$ salt of (a) $[Ni_{10}(SbEt)_2(CO)_{18}]^{2-}$ dianion (**4**), (b) $[Ni_{10}(Sb^iPr)_2(CO)_{18}]^{2-}$ dianion (**5**); (c) $[Ni_{10}(Sb^tBu)_2(CO)_{18}]^{2-}$ dianion (**6**), and (d) $[Ni_{10}(Sb(p\text{-}FC_6H_4))_2(CO)_{18}]^{2-}$ dianion (**7**).

antimony reagent needed to be coordinated to at least one halide ligand as well as an alkyl one; none of our attempts to react **1** with trialkylantimony reagents gave rise to any nickel−antimony carbonyl clusters. This necessity that the antimony reagents possess one or more halide ligands presumably stems from the driving force of its redox reaction with **1** being the formation of nickel(II) dihalide as a decomposition byproduct.

In this connection, Longoni and co-workers[36,37] reported that reactions of **1** with $SbCl_3$ led to the isolation of the highly intriguing $[Ni_{11}\{SbNi(CO)_3\}_2(CO)_{18}]^{n-}$ anions ($n = 2, 3, 4$) which contain a common Ni-centered 1,12-$Ni_{10}Sb_2$ icosahedral cage with a $Ni(CO)_3$ fragment coordinated as a Lewis-acid adduct to each of the two Sb atoms.

Structural Comparisons of $[Ni_{10}(SbR)_2(CO)_{18}]^{2-}$ (R = Me (3), Et (4), ^{i}Pr (5), ^{t}Bu (6), Ph (2), *p*-FC_6H_4 (7)). The crystallographically imposed centrosymmetric structure of the common empty 1,12-$Ni_{10}Sb_2$ cage in each of the six dianions can be described as a pentagonal antiprism of 10 surface Ni(*s*) atoms that is capped on the two pentagonal faces by SbR fragments. The essentially identical solid-state distribution of the 10 terminal and 8 bridging CO ligands about the $Ni_{10}Sb_2$ cage in each dianion reduces its pseudo symmetry from D_{5d} to C_{2h}-2/*m*.

Figures 1 and 2 reveal that the 10 terminal carbonyl ligands are each coordinated to a surface Ni(*s*) atom. The 8 bridging carbonyl ligands are arranged under pseudo-C_{2h} symmetry in alternating pairs of two mirror-related doubly bridging COs on adjacent interpentagonal edges and two triply bridging COs on adjacent

Table 1. Crystal Data, Data-Collection, and Refinement Parameters for $[NMe_4]^+_2[Ni_{10}(SbR)_2(CO)_{18}]^{2-}$ (R = Me (3), Et (4), ^{i}Pr(5), ^{t}Bu (6)·THF, *p*-FC_6H_4 (7)·THF) and for $Ni_2(CO)_4(\mu_2\text{-}Sb^tBu_2)$ (8)

	3	**4**	**5**	**6**	**7**	**8**
Crystal Data						
identification code						
formula	$C_{28}H_{30}N_2Ni_{10}O_{18}Sb_2$	$C_{30}H_{34}N_2Ni_{10}O_{18}Sb_2$	$C_{32}H_{38}N_2Ni_{10}O_{18}Sb_2$	$C_{42}H_{58}N_2Ni_{10}O_{20}Sb_2$	$C_{46}H_{48}F_2N_2Ni_{10}O_{20}Sb_2$	$C_{20}H_{36}Ni_2O_4Sb_2$
cryst color, habit	black block	black plate	dark brown prism	dark brown needle	reddish black plate	black block
cryst size (mm)	0.6 × 0.4 × 0.3	0.40 × 0.30 × 0.05	0.4 × 0.3 × 0.3	0.40 × 0.15 × 0.10	0.30 × 0.30 × 0.10	0.30 × 0.30 × 0.25
cryst system	monoclinic	triclinic	monoclinic	triclinic	triclinic	orthorhombic
space group	$P2_1/c$	$P\bar{1}$	$P2_1/c$	$P\bar{1}$	$P\bar{1}$	$P2_12_12$
unit cell dimens						
a (Å)	9.974(5)	9.99(1)	9.954(3)	10.843(6)	9.969(1)	8.712(2)
b (Å)	11.61(1)	11.33(2)	20.226(8)	11.616(6)	10.882(2)	12.281(2)
c (Å)	18.85(2)	11.52(1)	11.641(6)	13.501(6)	13.449(2)	12.340(2)
α (deg)	90	118.14(9)	90	110.43(4)	94.41(1)	90
β (deg)	95.03(6)	91.78(9)	91.70(3)	100.23(4)	92.90(1)	90
γ (deg)	90	92.22(10)	90	105.39(4)	93.34(1)	90
V (Å^3)	2175(3)	1147(2)	2343(2)	1466.0(13)	1449.9(4)	1320.3(4)
peaks to determine cell	20	25	20	25	43	20
temp (K)	123(2)	123(2)	123(2)	123(2)	148(2)	123(2)
wavelength (Å)	0.710 73	0.710 73	0.710 73	0.710 73	0.710 73	0.710 73
Z	2	1	2	1	1	2
fw	1513.14	1541.19	1569.24	1741.50	1817.46	701.40
D (calcd, g/cm^3)	2.311	2.231	2.225	1.973	2.08	1.764
abs coeff (mm^{-1})	5.509	5.224	5.119	4.103	4.158	3.448
F(000)	1476	754	1540	866	898	692
Data Collection						
diffractometer	Siemens $P\bar{1}$	Siemens P3/F	Siemens P3/F	Siemens P3/F	Siemens P4	Siemens P3/F
θ range for data collcn (deg)	2.70−25.00	2.01−25.00	2.01−25.07	2.98−25.02	1.52−22.50	2.34−25.03
index ranges	$-11 \le h \le 11$	$-11 \le h \le 11$	$-11 \le h \le 11$	$-12 \le h \le 12$	$-10 \le h \le 10$	$-10 \le h \le 0$
	$-13 \le k \le 13$	$-13 \le k \le 13$	$0 \le k \le 24$	$-12 \le k \le 13$	$-11 \le k \le 11$	$-14 \le k \le 0$
	$-22 \le l \le 22$	$-13 \le l \le 13$	$0 \le l \le 13$	$-16 \le l \le 0$	$-14 \le l \le 14$	$-14 \le l \le 0$
scan type	Wyckoff ω	Wyckoff ω	Wyckoff ω	Wyckoff ω	Wyckoff ω	Wyckoff ω
scan speeds (deg/min)	variable, 3−15	variable, 2−12	variable, 2−12	variable, 3−30	variable, 3−30	variable, 3−30
scan range (deg in ω)	0.4	0.4	1.0	0.8	0.82	0.4
no. check reflcns/freq	3/47	3/47	3/47	3/97	3/97	3/47
no. of reflcns collcd	11273	4589	4446	5365	7512	1368
no. of indepdt reflcns	3823 (R_{int} = 0.054)	4034 (R_{int} = 0.054)	4137 (R_{int} = 0.056)	5132 (R_{int} = 0.042)	3777 (R_{int} = 0.028)	1368 (R_{int} = 0.00)
Solution and Refinement						
weighting scheme a, b[a]	0.0304, 4.1784	0.0911, 0	0.0863, 0	0.0718, 2.0358	0.0637, 0.6305	0.0400, 0
data/restraints/parameters	3823/10/273	4033/10/281	4136/10/290	5132/0/343	3776/0/370	1368/0/128
goodness-of-fit on F^2	1.087	0.944	0.982	1.035	1.038	1.054
final R indices [$I > 2\sigma(I)$][b]	$R_1(F) = 0.036$	$R_1(F) = 0.071$	$R_1(F) = 0.052$	$R_1(F) = 0.043$	$R_1(F) = 0.031$	$R_1(F) = 0.034$
	$wR_2(F^2) = 0.084$	$wR_2(F^2) = 0.15$	$wR_2(F^2) = 0.13$	$wR_2(F^2) = 0.11$	$wR_2(F^2) = 0.084$	$wR_2(F^2) = 0.071$
R indices (all data)[b]	$R_1(F) = 0.046$	$R_1(F) = 0.12$	$R_1(F) = 0.079$	$R_1(F) = 0.054$	$R_1(F) = 0.034$	$R_1(F) = 0.045$
	$wR_2(F^2) = 0.089$	$wR_2(F^2) = 0.17$	$wR_2(F^2) = 0.14$	$wR_2(F^2) = 0.12$	$wR_2(F^2) = 0.092$	$wR_2(F^2) = 0.076$
obsd data [$I > 2\sigma(I)$]	3139	2317	2895	4286	3531	1164
largest diff peak and hole (e Å^{-3})	1.067 and −0.505	1.093 and −1.174	1.469 and −1.047	1.338 and −0.862	0.826 and −0.783	0.767 and −0.651
largest and mean Δ/esd	0.000 and 0.000	−0.001 and 0.000	0.002 and 0.000	0.001 and 0.000	0.002 and 0.000	0.002 and 0.000

[a] $w = 1/[\sigma^2(F_o^2) + (aP)^2 + bP]$; $P = [F_o^2 + 2F_c^2]/3$. [b] $R_1(F) = \sum||F_o| - |F_c||/\sum|F_o|$; $wR_2(F^2) = [\sum[w_i(F_o^2 - F_c^2)^2]/\sum[w_i(F_o^2)^2]]^{1/2}$.

Table 2. Selected Interatomic Distances for the *closo*-1,12-Disubstituted Icosahedral $Ni_{10}Sb_2$ Core in the Centrosymmetric $[Ni_{10}(SbR)_2(CO)_{18}]^{2-}$ Dianion, as $[NMe_4]^+$, Where R = Me (3), Et (4), ^{i}Pr (5), ^{t}Bu (6), Ph (2),[29] and *p*-FC_6H_4 (7)

	compd no. (R)					
dist	**3** (Me)	**4** (Et)	**5** (^{i}Pr)	**6** (^{t}Bu)	**2** (Ph)	**7** (*p*-FC_6H_4)
	A. Distance between Centrosymmetrically Related Core Atoms					
Ni(1)−Ni(1a)	5.235(4)	5.245(8)	5.195(3)	5.173(3)	5.163(2)	5.161(1)
Ni(2)−Ni(2a)	5.142(3)	5.215(7)	5.162(3)	5.118(5)	5.131(2)	5.103(1)
Ni(3)−Ni(3a)	5.194(5)	5.180(7)	5.133(3)	5.158(3)	5.167(2)	5.162(1)
Ni(4)−Ni(4a)	5.184(3)	5.168(7)	5.129(3)	5.152(4)	5.151(2)	5.168(1)
Ni(5)−Ni(5a)	5.153(3)	5.149(6)	5.167(3)	5.108(3)	5.147(2)	5.157(1)
Ni−Ni (av)	5.18(av)	5.19(av)	5.16(av)	5.14(av)	5.15(av)	5.15(av)
Sb(1)−Sb(1a)	3.848(3)	3.904(7)	3.944(2)	4.159(2)	3.905(2)	3.884(1)
	B. Nickel−Antimony Distances					
Sb−Ni(1)	2.576(2)	2.568(4)	2.556(2)	2.581(2)	2.556(1)	2.554(1)
Sb−Ni(2)	2.538(2)	2.576(3)	2.573(2)	2.573(2)	2.543(1)	2.541(1)
Sb−Ni(3)	2.575(2)	2.557(4)	2.551(2)	2.572(1)	2.553(1)	2.553(1)
Sb−Ni(4)	2.563(2)	2.577(4)	2.549(1)	2.577(2)	2.541(1)	2.529(1)
Sb−Ni(5)	2.538(2)	2.570(3)	2.570(2)	2.587(2)	2.556(1)	2.548(1)
Sb−Ni (av)	2.56(av)	2.57(av)	2.56(av)	2.58(av)	2.55(av)	2.54(av)
	C. Intrapentagonal Nickel−Nickel Distances					
Ni(1)−Ni(2)	2.873(2)	2.906(4)	2.892(2)	2.851(2)	2.868(1)	2.852(1)
Ni(2)−Ni(3)	2.709(2)	2.745(4)	2.694(2)	2.673(2)	2.681(1)	2.675(1)
Ni(3)−Ni(4)	2.856(2)	2.798(4)	2.787(2)	2.789(2)	2.816(1)	2.823(1)
Ni(4)−Ni(5)	2.731(2)	2.708(4)	2.689(2)	2.689(2)	2.679(1)	2.681(1)
Ni(5)−Ni(1)	2.863(2)	2.895(4)	2.880(2)	2.839(3)	2.881(1)	2.888(1)
Ni−Ni(av)	2.81(av)	2.81(av)	2.79(av)	2.77(av)	2.79(av)	2.78(av)
	D. Interpentagonal Nickel−Nickel Distances					
Ni(1)−Ni(3a)	2.519(2)	2.530(5)	2.516(2)	2.558(2)	2.514(1)	2.516(1)
Ni(1)−Ni(4a)	2.516(2)	2.524(4)	2.526(2)	2.553(2)	2.514(1)	2.523(1)
Ni(2)−Ni(4a)	2.525(2)	2.541(5)	2.538(2)	2.571(2)	2.548(1)	2.545(1)
Ni(2)−Ni(5a)	2.414(2)	2.376(4)	2.366(2)	2.390(2)	2.366(1)	2.361(1)
Ni(3)−Ni(5a)	2.507(2)	2.555(5)	2.547(2)	2.553(2)	2.546(1)	2.542(1)
Ni−Ni(av)	2.50(av)	2.51(av)	2.50(av)	2.53(av)	2.50(av)	2.50(av)

triangular faces formed by one intrapentagonal and two interpentagonal edges. Of the 10 *interpentagonal* Ni(*s*)−Ni(*s*′) edges, four are each linked by a doubly bridging CO, four each linked by one triply bridging CO, and two each linked by two triply bridging COs. Of the 10 *intrapentagonal* Ni(*s*)−Ni(*s*′) edges, four are each connected by one triply bridging CO, while the other six edges are not spanned by any carbonyl linkages. Thus, the 10 terminal, 4 doubly bridging, and 4 triply bridging COs combine to form 30 carbonyl links such that each surface Ni(*s*) is analogously connected to one terminal and two bridging COs. This particular pseudo-C_{2h} arrangement of the carbonyl ligands enables each of the 10 Ni(*s*) atoms in a given dianion to possess an analogous negative charge density in accordance with its spectroscopic behavior. Nevertheless, an examination of Table 2 reveals the following interrelationships among the empty $Ni_{10}Sb_2$ icosahedral cages of the six dianions:

(1) Each icosahedral cage is similarly distorted from a regular one of I_h symmetry (*e.g.*, $[B_{12}H_{12}]^{2-}$) by a large oblate compression along the pseudo 5-fold nonbonding Sb···Sb′ axis. The extent of this deformation varies in a systematic fashion with the size of the antimony-attached alkyl substituent, as reflected by the observed variations in the Sb···Sb′ distances for the four alkyl derivatives—*viz.*, R = Me (3.848(3) Å), R = Et (3.904(7) Å), R = ^{i}Pr (3.944(2) Å), R = ^{t}Bu (4.159(2) Å). The corresponding D_{5d} cage compressions for the phenyl and *p*-fluorophenyl substituents are expectedly analogous, as evidenced by similar Sb···Sb′ distances of 3.905(2) and 3.883(1) Å, respectively. These distinct variations can be readily attributed to steric effects of the 20-vertex ligand polyhedron in that an increased cage size along the pseudo 5-fold Sb···Sb′ axis would decrease repulsions between the larger R substituents and adjacent carbonyl ligands. The corresponding alterations in the mean nonbonding Ni···Ni′ distances among the five centrosymmetrically related pairs of Ni(*s*) atoms are small upon change of the R substituent—*viz.*, R = Me (5.18 Å), R = ^{t}Bu (5.14 Å), R = Ph (5.15 Å), R = *p*-FC_6H_4 (5.15 Å). The extent of the oblate D_{5d} compression within each 1,12-$Ni_{10}Sb_2$ cage as a function of R can be roughly estimated by the ratio of the Sb···Sb′ distance to the mean Ni···Ni′ distance; the ratios vary from 0.74 for R = Me to 0.81 for R = ^{t}Bu.

(2) The five independent Ni−Sb distances within one Sb-capped nickel pentagon vary from 2.56 Å (av) for R = Me to 2.58 Å (av) for ^{t}Bu and from 2.54 Å (av) to 2.55 Å (av) for the two aryl derivatives.

(3) The five independent *intrapentagonal* Ni−Ni′ distances within one Sb-capped nickel pentagon decrease in a small but uniform fashion from 2.81 Å (av) for R = Me to 2.77 Å (av) for R = ^{t}Bu; this trend is a necessary consequence of the 0.31 Å elongation of the cage along the pseudo 5-fold Sb···Sb′ axis upon the change from R = Me to R = ^{t}Bu, because the corresponding mean Ni−Sb distance has increased by only 0.02 Å from R = Me to R = ^{t}Bu.

(4) The five independent *interpentagonal* Ni−Ni′ distances between the two centrosymmetrically related Sb-capped pentagons are 2.50 Å (av) for R = Me, Et, Ph, and *p*-FC_6H_4, 2.51 Å (av) for R = ^{i}Pr, and 2.53 Å (av) for R = ^{t}Bu; the largest mean distance for R = ^{t}Bu is also consistent with the cage elongation along the pseudo 5-fold Sb···Sb′ axis. The observation that these mean *interpentagonal* edges are 0.3 Å smaller than the mean *intrapentagonal* edges is ascribed to the marked

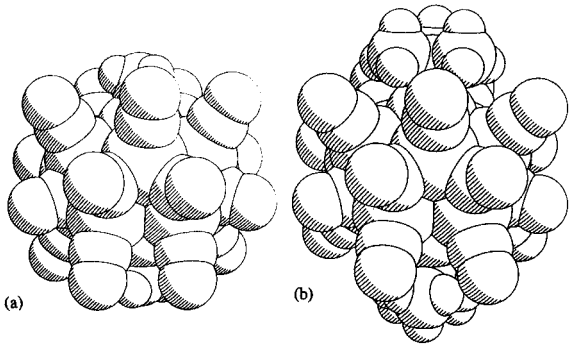

Figure 3. Space-filling model of (a) $[Ni_{10}(SbMe)_2(CO)_{18}]^{2-}$ (**3**) and (b) $[Ni_{10}(Sb^tBu)_2(CO)_{18}]^{2-}$ (**6**). The much bulkier Sb-attached *tert*-butyl substituents in **6** relative to the methyl substituents in **3** produce a much greater bending (by *ca.* 12°) of the five similarly oriented independent terminal COs away from the adjacent ^{t}Bu substituent bound to the capped Sb atom.

bond-length shortening effects of the bridging carbonyl ligands which span all of the interpentagonal edges.

(5) Another trend that can be observed from an increase in size of the alkyl ligand is the steric consequence on the angular disposition of the 10 terminal carbonyls. The estimated cone angles of the methyl and *tert*-butyl substituents are 58 and 96°, respectively; the resulting mean observed angle between the five similarly disposed terminal COs out of the mean plane of the five *intrapentagonal* Ni(*s*) atoms (to which they are coordinated) varies from *ca.* 60° for R = Me (**3**) to *ca.* 48° for R = ^{t}Bu (**6**); intermediate angular values of 56 and 54° were estimated for R = Et (**4**) and R = ^{i}Pr (**5**), respectively. Figure 3 compares the space-filling models of **3** and **6** which clearly show a greater angular bending of the terminal carbonyl ligands away from the ^{t}Bu substituents in **6** due to their much greater steric demands. Hence, the different angular arrangement of the terminal COs and the cage elongation for R = ^{t}Bu are sterically-driven effects.

(6) Changing the electronegativity of the two substituents bound to each antimony does not have any noticeable effect on the structure. Although the *p*-FC_6H_4 substituent is more electron-withdrawing than the Ph one, there are no significant observable geometrical differences between R = *p*-FC_6H_4 (**7**) and the previously characterized phenylstibinidene $[Ni_{10}(SbPh)_2(CO)_{18}]$ dianion (**2**).[29]

A geometrical comparison of the $[Ni_{10}(SbMe)_2(CO)_{18}]^{2-}$ dianion containing an empty 1,12-$Ni_{10}Sb_2$ cage with the crystallographically determined $[Ni_{11}\{SbNi(CO)_3\}_2(CO)_{18}]^{n-}$ anions (n = 2, 3) containing a common Ni-centered 1,12-$Ni_{10}Sb_2$ cage is given in the following paper[34] on the homologous $[Ni_{10}(EMe)_2(CO)_{18}]^{2-}$ dianions (E = P, As, Sb, Bi).

Experimental Analyses of the $[Ni_{10}(SbR)_2(CO)_{18}]^{2-}$ Dianions (E = Me (3), Et (4), ^{i}Pr (5), ^{t}Bu (6), Ph (2), *p*-FC_6H_4 (7)) and Resulting Implications. (a) Infrared Spectral Analyses. The strong absorption band due to the terminal carbonyl ligands for **3**−**6** in THF solutions was observed within a narrow range of 2004−2007 cm^{-1}, which is within experimental error. A larger range from 1834 cm^{-1} for **3** to 1817 cm^{-1} for **6** was found for the doubly bridging carbonyl band in these four clusters with antimony-attached alkyl substituents. The terminal carbonyl band for each of the two clusters containing aryl substituents was observed at a somewhat higher frequency—*viz.*, at 2020 cm^{-1} for **2** and at 2017 cm^{-1} for **7**. Although the IR band for the triply bridging carbonyl ligands was observed as a weak maximum for **2** and for **7**, for the other clusters with alkyl substituents this band was either detected as a shoulder of a broad edge-bridged carbonyl band or not observed.

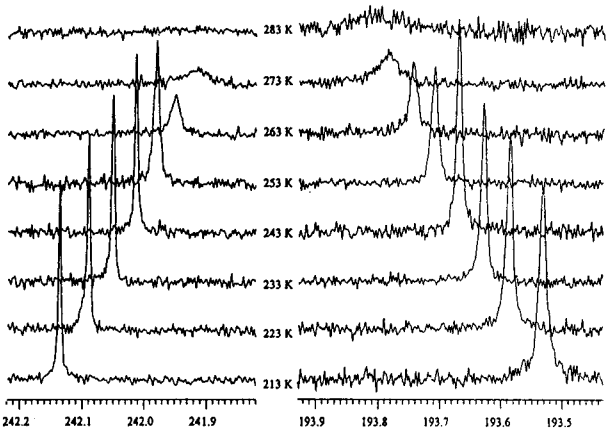

Figure 4. Stack plot within the terminal/bridging carbonyl range of $^{13}C\{^1H\}$ NMR spectra of $[Ni_{10}(Sb^iPr)_2(CO)_{18}]^{2-}$ (**5**) from 213 to 283 K at 10 °C intervals. The two sharp resonances at 242.1 and 193.5 ppm observed in the slow-exchange $^{13}C\{^1H\}$ spectrum at 213 K were assigned to the 8 bridging and 10 terminal carbonyl carbons, respectively.

(b) Electrochemical Analysis. Cyclic voltammograms of **3** and **5** in acetonitrile solutions did not exhibit any reversible reduction out to −2.0 V. However, both of these CVs exhibited an irreversible wave at *ca.* E_p = +0.60 V, which indicates that each cluster undergoes either a significant rearrangement or decomposition at this potential. The relatively small variations in CV (as well as in IR) data indicate no marked changes in electron-density surface charge on the $Ni_{10}Sb_2$ icosahedral cage arising from the formal substitution of alkyl and aryl groups bound to the antimony atoms.

(c) NMR Spectral Analysis. Room-temperature $^{13}C\{^1H\}$ NMR spectra of $[NMe_4]_2$[**3**] and $[NMe_4]_2$[**5**] in acetone-d_6 exhibited signals due to the methyl groups in the counterions and the antimony-bound alkyl groups; the failure to observe resonances due to the carbonyl ligands is consistent with rapid CO(bridging)/CO(terminal) exchange. However, at lower temperatures two additional resonances appeared due to the carbonyl ligands (Figure 4); at −60 °C these observed signals for **3** (and for **5**) at δ 240.8 (242.1) and 191.8 (193.5) ppm have been assigned to the bridging and terminal carbonyls, respectively. This assignment is consistent with that previously made for the methylphosphinidene homologue, $[Ni_{10}(PMe)_2(CO)_{18}]^{2-}$, for which a similar limiting slow-exchange $^{13}C\{^1H\}$ NMR spectrum at −60 °C consisted of two sharp resonances for the bridging and terminal COs at 240.0 and 188.7 ppm, respectively.[59] This assignment is also consistent with those based upon limiting slow-exchange $^{13}C\{^1H\}$ spectra obtained at −80 °C and interpreted by Longoni, Heaton, and Chini[60] for several nickel carbonyl clusters; resonances assigned to terminal COs ranged from 192 to 203 ppm, while those assigned to the doubly bridging COs ranged from 230 to 257 ppm.

(59) Gavney, J. A., Jr., Ph.D. Thesis, University of Wisconsin—Madison, 1992.

(60) Longoni, G.; Heaton, B.; Chini, P. *J. Chem. Soc., Dalton Trans.* **1980**, 1537−1541.

Although the X-ray crystal structures of the $Ni_{10}Sb_2$ dianions including **3** and **5** established that in the solid state there are four doubly bridging (μ_2) and four triply bridging (μ_3) COs, in solution these correspond to only a single resonance at −60 °C. This nonsurprising observation provides definite evidence that in solution the doubly and triply bridging carbonyl ligands are still fluxional at −60 °C. The fluxional process involving exchange of the bridging and terminal carbonyl ligands was investigated for **5** on the NMR time scale at temperatures above −26 °C (Figure 4). The two signals at 242.1 and 193.5 ppm were sharp below this temperature (*i.e.*, the natural peak widths at half-heights under our experimental conditions were *ca.* 0.70 and 1.45 Hz, respectively); at higher temperatures, these two peaks broadened and eventually became indistinguishable from the baseline (Figure 4). On the basis of the lineshape analysis[61] of the variable-temperature $^{13}C\{^1H\}$ spectra of **5**, an activation energy, E_a, of 52.5 kJ/mol for the bridging/terminal carbonyl exchange process was estimated.

(d) Mass Spectral Analysis. A negative-ion ESI mass spectrum of $[NMe_4]_2$[**5**] exhibited 12 high-range m/z signals corresponding to doubly charged ion-fragments. The assignment of each ion-fragment formula was based upon the resulting simulated isotopic pattern matching the observed one for each signal.[62] The observed isotopic pattern for one signal corresponds to the doubly charged ion-parent, $[Ni_{10}(Sb^iPr)_2(CO)_{18}]^{2-}$ (**5**), denoted as M^{2-}; those for four signals correspond to $[M - nCO]^{2-}$ ions (n = 1, 2, 3, 4), those for 6 observed signals correspond to $[M - nCO - 2C_3H_7]^{2-}$ ions (n = 3, 4, 5, 6, 7, 8), and that for one signal corresponds to the $[M - 4CO - 1C_3H_7]^{2-}$ ion.

The observance in the ESI mass spectrum of the doubly charged ion-parent, M^{2-}, and the other assigned ion-fragment formulas is completely compatible not only with the stoichiometry of the dianion (**5**) but also with the expected ion-fragmentation pattern based upon the relative bond energies. The fact that all of these high-range signals correspond to $Ni_{10}Sb_2$-containing ion-fragments indicates that the $Ni_{10}Sb_2$ icosahedral cage is relatively stable to degradation. The detection of one signal for the $[M - 4CO - 1C_3H_7]^{2-}$ ion-fragment versus 6 signals for the $[M - nCO - 2C_3H_7]^{2-}$ ion-fragments (n = 3−8) and 4 signals for the $[M - nCO]^{2-}$ ones (n = 1−4) is consistent with the bond dissociation energies of the Ni−CO and Sb−C_3H_7 bonds being similar.

The large number of observed high-range signals including the weak ion-parent one for the dianion (**5**) illustrates the immense capability of the ESI process in placing a nonvolatile ionic compound into the gas phase generally without fragmentation for mass spectral analysis.[63]

$Ni_2(CO)_4(\mu_2\text{-}Sb^tBu_2)_2$ (8). (a) Structural/Bonding Features. This yellow-brown neutral dimer was isolated as a side product in approximately 10% yield by column chromatography from the hexane extract of the resulting reaction of **1** with $^tBu_2SbCl$, from which the $[Ni_{10}(Sb^tBu)_2(CO)_{18}]^{2-}$ dianion was obtained as the major Ni−Sb product.

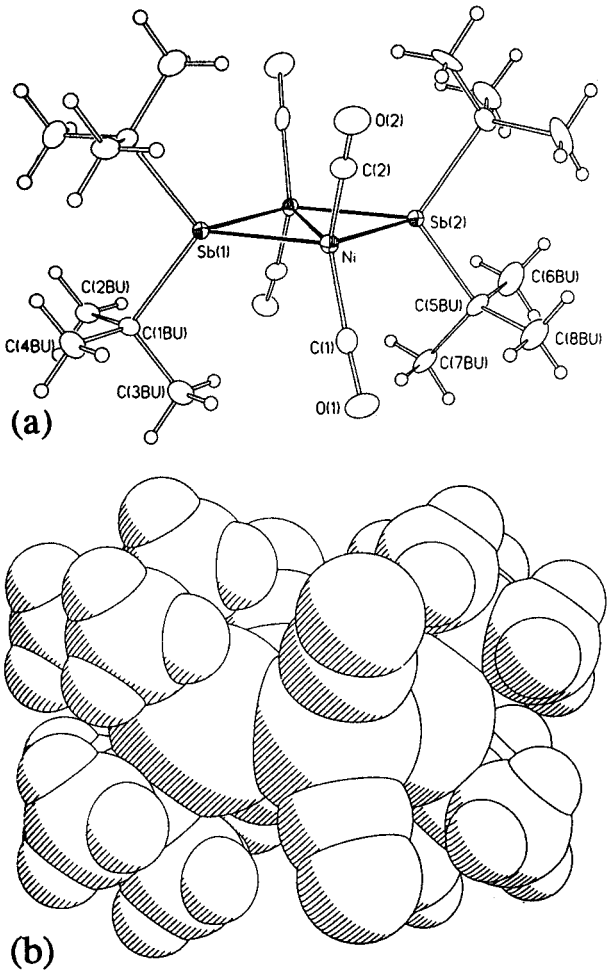

Figure 5. (a) View of the neutral $Ni_2(CO)_4(\mu_2\text{-}Sb^tBu_2)_2$ (**8**). This 34-electron dimer lies on a crystallographic 2-fold axis that passes through the two Sb atoms; the independent non-hydrogen atoms are labeled. Ni−Sb−Ni′ bond angles: 68.4(1) and 68.5(1)°. Ni−Ni′ bonding interaction: 2.757(2) Å. (b) Space-filling model of this molecular dimer which shows the spatial coverage of the bulky antimony-attached *tert*-butyl substituents that protect the two Ni(I) atoms.

This dimer (Figure 5) lies on a crystallographic 2-fold axis that passes through both antimony atoms. Each symmetry-equivalent Ni atom is coordinated to two carbonyl ligands and to two Sb atoms at the corners of a somewhat distorted tetrahedron, as evidenced by the OC−Ni−CO′ and Sb−Ni−Sb′ bond angles of 119.1(4) and 111.54(4)°, respectively, being considerably larger than the four Sb−Ni−CO bond angles of 106.6(av) and range 105.0(3)−108.6(3)°. The dimeric configuration of pseudo D_{2h}-*2/m 2/m 2/m* symmetry formally arises from the fusion of the two identical tetrahedral-like $(OC)_2Ni(Sb^tBu_2)_2$ units along the common nonbonding $^tBu_2Sb\cdots Sb^tBu_2$ edge of 4.053(1) Å. The resulting two Ni and two bridging Sb atoms form a rhombus core with crystallographically independent Ni−Sb bond lengths of 2.449(1) and 2.452(1) Å. The existence of a direct Ni−Ni′ electron-pair bond in this 34-electron dimer is supported by both the relatively short Ni−Ni′ distance of 2.757(2) Å and the sharply acute Ni−Sb−Ni′ bond angles of 68.40(6) and 68.51(6)°.

To our knowledge, $Ni_2(CO)_4(\mu_2\text{-}Sb^tBu_2)_2$ is the first example of a stibinido-bridged dimer corresponding to the known 34-electron $Ni_2(CO)_4(\mu_2\text{-}PR_2)_2$-type dimer with two tetrahedral-like Ni(I) atoms linked by a Ni−Ni bond (R = Ph,[44] Cy,[64] ^tBu[45]). Other isostructural and

(61) WinDNMR: Dynamic NMR Spectra for Windows: (a) Reich, H. J. *J. Chem. Educ.: Software* **1995**, *3D*, No. 2. (b) Reich, H. J. *J. Chem. Educ.* **1995**, *72*, 1086.
(62) Arnold, L. *Isotope Pattern Calculator*, Version 1.6, 1990.
(63) (a) Hop, C. E. C. A.; Bakhliar, R. *J. Chem. Educ.* **1996**, *73*, A162−169 and references therein. (b) Hop, C. E. C. A.; Saulys, D. A.; Gaines, D. F. *Inorg. Chem.* **1995**, *34*, 1977−1978.

Table 3. Intramolecular Distances and Bond Angles for $Ni_2(CO)_4(\mu_2\text{-}Sb^tBu_2)_2$ (8)

Bond Lengths (Å)			
Sb(1)−C(1Bu)	2.183(10)	Sb(2)−Ni	2.449(1)
Sb(1)−C(1Bu)′	2.183(10)	Sb(2)−Ni′	2.449(1)
Sb(1)−Ni′	2.452(1)	Ni−C(1)	1.768(8)
Sb(1)−Ni	2.452(1)	Ni−C(2)	1.787(8)
Sb(2)−C(5Bu)	2.216(11)	Ni−Ni′	2.757(2)
Sb(2)−C(5Bu)′	2.216(11)		
Bond Angles (deg)			
C(1Bu)−Sb(1)−C(1Bu)′	107.4(5)	C(1)−Ni−Sb(2)	105.2(3)
C(1Bu)−Sb(1)−Ni′	118.1(3)	C(2)−Ni−Sb(2)	107.5(3)
C(1Bu)′−Sb(1)−Ni′	120.6(3)	C(1)−Ni−Sb(1)	108.6(3)
C(1Bu)−Sb(1)−Ni	120.6(3)	C(2)−Ni−Sb(1)	105.0(3)
C(1Bu)′−Sb(1)−Ni	118.1(3)	Sb(2)−Ni−Sb(1)	111.54(4)
Ni′−Sb(1)−Ni	68.40(6)	C(1)−Ni−Ni′	121.1(3)
C(5Bu)−Sb(2)−C(5Bu)′	108.1(6)	C(2)−Ni−Ni′	119.8(3)
C(5Bu)−Sb(2)−Ni	118.8(3)	Sb(2)−Ni−Ni′	55.75(3)
C(5Bu)′−Sb(2)−Ni	119.3(3)	Sb(1)−Ni−Ni′	55.80(3)
C(5Bu)−Sb(2)−Ni′	119.3(3)	O(1)−C(1)−Ni	175.2(9)
C(5Bu)′−Sb(2)−Ni′	118.8(3)	O(2)−C(2)−Ni	173.8(8)
Ni−Sb(2)−Ni′	68.51(6)		
C(1)−Ni−C(2)	119.1(4)		

electronically equivalent $Ni_2L_4(\mu_2\text{-}ER_2)_2$ molecules include $Ni_2(PMe_3)_4(\mu_2\text{-}P(H^tBu)_2)_2$[46] and $Ni_2(CNC_6H_4Me)_4(\mu_2\text{-}As^tBu_2)_2$.[51]

In our earlier work[29] which resulted in the synthesis and stereophysical characterization of the $[Ni_{10}(SbPh)_2(CO)_{18}]^{2-}$ dianion (**2**), we also isolated and structurally characterized a side product, $Ni_2(CO)_4(\mu_2\text{-}Ph_2SbOSbPh_2)_2$, containing a centrosymmetric eight-membered $(NiSbOSb)_2$ ring. At that time we stated that it is not surprising that no stibinido-bridged analogue of the $Ni_2(CO)_4(\mu_2\text{-}PR_2)_2$-type dimer is known in that any such $Ni_2(\mu_2\text{-}SbR_2)_2$ species would be much more unstable on the basis of both electronic and steric effects. We then pointed out that "in addition to the considerably weaker coordinating ability of the less basic Sb(III) donor atoms relative to P(III) donor atoms,[65,66] intramolecular steric pressures would presumably preclude the existence of any hypothetical *cyclo*-Ni_2Sb_2 dimer due to the considerably larger Sb atoms imposing a much greater angular strain upon the four-membered Ni_2Sb_2 ring containing an electron-pair Ni−Ni′ bonding interaction."

From our comparative structural/bonding analysis of **8** with other closely related, crystallographically determined nickel dimers (presented below), we now realize that the necessary molecular component that led to our success in isolating **8** as a stable entity is the presence on each Sb atom of two bulky ^{t}Bu substituents which protect the Ni−Ni-bonded Ni_2Sb_2 ring containing two tetrahedral-like Ni(I) from air oxidation (*vide infra*).

(b) Geometrical Comparison with Closely Related $Ni_2(\mu_2\text{-}ER_2)_2$ Dimers (E = P, As) Containing Ni_2E_2 Rings (with and without Ni−Ni′ Electron-Pair Coupling Interactions) and Resulting Bonding Implications. Table 4 provides a comparison of the mean geometric parameters of **8** with those of the 36-electron $Ni_2Cp_2(\mu_2\text{-}PPh_2)_2$[67] and of four other isostructural 34-electron $Ni_2L_4(\mu_2\text{-}ER_2)_2$ (E = P, As), for which L denotes a two-electron donor (*viz.*, CO, PMe_3, CNC_6H_4Me).[44−46,51] Table 4 also presents the mean geometric parameters of two 32-electron $Ni_2L_3(\mu_2\text{-}PR_2)_2$[47] and four 30-electron $Ni_2L_2(\mu_2\text{-}ER_2)_2$ (E = P, As).[48−51] In each 34-electron dimer including **8**, two tetrahedral-like Ni(I) are joined by a Ni−Ni′ bond corresponding to an electron-pair coupling of a 17e−17e system. In each 32-electron dimer a trigonal planar-like Ni(I) and a tetrahedral-like Ni(I) are linked by a Ni−Ni′ bond that corresponds to an electron-pair coupling of a 15e−17e system, while in each 30-electron dimer two trigonal planar-like Ni(I) are connected by a Ni−Ni′ bond that corresponds to a 15e−15e electron-pair coupling.

Several important structural/bonding points emerge from a comparative analysis of the molecular parameters for these dimers. First, the crystallographic data reinforce the hypothesis that the observed severe angular deformation of the planar Ni_2E_2 rhombus in each of these 34-, 32-, and 30-electron dimers is caused by a strong direct Ni−Ni′ electron-pair bond instead of an intramolecular antiferromagnetic ligand-bridged exchange coupling (which is presumed to exert only a small influence on the molecular geometry). Thus, a strong Ni−Ni′ bonding interaction accounts for the sharply acute Ni−E−Ni′ bond angles of range 65−72° in the Ni_2E_2 rhombus of each of the 11 metal−metal-bonded dimers listed in Table 4; in contrast, normal Ni−E−Ni′ bond angles of 102.4° are observed in the Ni_2P_2 rhombus of the 36-electron $Ni_2Cp_2(\mu_2\text{-}PPh_2)_2$, for which the nonbonding Ni···Ni′ distance of 3.36 Å signifies no Ni−Ni′ bond between the two Ni(II) atoms.[67]

Second, Table 4 reveals that the view of a direct Ni−Ni′ bonding interaction of considerable strength in all five of the 34-electron $Ni_2L_4(\mu_2\text{-}ER_2)_2$ dimers (E = P, As, Sb) is strongly supported by the similar acute Ni−E−Ni′ bond angles of range 69.9−72.2° for E = P, 71.3° for E = As, and 68.5° for E = Sb. This angular invariance with a change of the bridging E atoms from P to As and then to Sb signifies that the sizable increases in Ni−Ni′ bonding distances from 2.51 Å in $Ni_2(CO)_4(\mu_2\text{-}PR_2)_2$ (R = Ph,[44] ^{t}Bu[45]) to 2.69 Å in $Ni_2(CNC_6H_4Me)_4(\mu_2\text{-}As^tBu_2)_2$[51] and then to 2.76 Å in $Ni_2(CO)_4(\mu_2\text{-}Sb^tBu_2)_2$ are primarily due to an increased size effect of the bridging E atoms; the fact that the terminal *p*-tolyl isocyanide ligands in the arsenic-bridged dimer are not nearly as strongly π-back-bonding as the terminal carbonyl ligands in the phosphorus- and antimony-bridged dimers would presumably give rise to a more negative charge density on each Ni(I) and thereby would expectedly result in a longer Ni−Ni′ distance and correspondingly larger Ni−E−Ni′ bond angles, as observed.

Third, Table 4 shows that the Ni−Ni′ distances in the three 30-electron phosphorus-bridged dimers are *ca.* 0.03−0.05 Å shorter than those in the two 32-electron phosphorus-bridged dimers, which in turn are *ca.* 0.06−0.10 Å shorter than those in the three 34-electron phosphorus-bridged dimers. Likewise, the Ni−Ni′ distance in the 30-electron $Ni_2(PMe_3)_2(\mu_2\text{-}As^tBu_2)_2$[51] is 0.26 Å shorter than that in the 34-electron $Ni_2(CNC_6H_4Me)_4(\mu_2\text{-}As^tBu_2)_2$.[51] These distinct bond-length variations are consistent with (1) two coordinatively-unsaturated trigonal planar-like Ni(I) in each 30-electron dimer forming a stronger and hence shorter Ni−Ni′ bonding interaction than that between a trigonal planar-like Ni(I) and a tetrahedral-like Ni(I) in each 32-electron dimer and (2) the Ni−Ni′ bonding interaction in each 32-electron dimer being similarly stronger and thereby

(64) Nobile, C. F.; Vasapollo, G.; Giannoccaro, P.; Sacco, A. *Inorg. Chim. Acta* **1981**, *48*, 261−263.
(65) Booth, G. *Adv. Inorg. Chem. Radiochem.* **1964**, *6*, 1−69.
(66) Doak, G. O.; Freeman, L. D. *Organometallic Compounds of Arsenic, Antimony, and Bismuth*; Wiley-Interscience: New York; 1970, pp 1−16 and references therein.
(67) Coleman, J. M.; Dahl, L. F. *J. Am. Chem. Soc.* **1967**, *89*, 542−552.

Table 4. Comparison of Mean Geometric Parameters of 36-Electron $Ni_2Cp_2(\mu_2\text{-}ER_2)_2$ (E = P), 34-Electron $Ni_2L_4(\mu_2\text{-}ER_2)_2$ (E = P, As, Sb), 32-Electron $Ni_2L_3(\mu_2\text{-}ER_2)_2$ (E = P), and 30-Electron $Ni_2L_2(\mu_2\text{-}ER_2)_2$ (E = P, As) Dimers Containing Planar Four-Membered Heterocyclic Ring Ni_2E_2 Systems with and without Ni−Ni Electron-Pair Bonding Interactions

compd	ref	CVE	Ni−Ni (Å)	Ni−E (Å)	E···E (Å)	Ni−E−Ni′ (deg)	E−Ni−E′ (deg)
				Ni_2P_2 Core			
$Ni_2Cp_2(\mu_2\text{-}PPh_2)_2$	67	36[a]	3.36	2.16	2.70	102.4	77.6
$Ni_2(CO)_4(\mu_2\text{-}PPh_2)_2$	44	34[b]	2.51	2.19	3.60	69.9	110.1
$Ni_2(CO)_4(\mu_2\text{-}P^tBu_2)_2$	45	34[b]	2.51	2.20	3.62	69.4	110.6
$Ni_2(PMe_3)_4(\mu_2\text{-}PH^tBu)_2$	46	34[b]	2.56	2.18	3.52	72.2	107.8
$Ni_2(CO)_3(\mu_2\text{-}P^tBu_2)_2$	47	32[c]	2.41	2.20	3.68	66.5	113.5
$Ni_2(CO)_2(PMe_3)(\mu_2\text{-}P^tBu_2)_2$	47	32[c]	2.45	2.15	3.54	67.5	112.5
$Ni_2(PMe_3)_2(\mu_2\text{-}P(SiMe_3)_2)_2$	48	30[d]	2.38	2.19	3.60	66.0	114.0
$Ni_2(PMe_3)_2(\mu_2\text{-}P^tBu_2)_2$	49	30[d]	2.38	2.16	3.60	66.2	113.8
$Ni_2(C_2H_4)_2(\mu_2\text{-}PCy_2)_2$	50	30[d]	2.39	2.15	3.57	67.6	112.4
				Ni_2As_2 Core			
$Ni_2(CNC_6H_4Me)_4(\mu_2\text{-}As^tBu_2)_2$	51	34[b]	2.69	2.31	3.76	71.3	108.7
$Ni_2(PMe_3)_2(\mu_2\text{-}As^tBu_2)_2$	51	30[d]	2.43	2.27	3.82	64.9	115.1
				Ni_2Sb_2 Core			
$Ni_2(CO)_4(\mu_2\text{-}Sb^tBu_2)_2$	*f*	34[b]	2.76	2.45	4.05	68.5	111.5

[a] 18 e−18 e system: No Ni−Ni bonding interaction between two Ni(II) atoms. [b] 17 e−17 e system: Electron-pair coupling between two tetrahedral-like Ni(I) atoms. [c] 15 e−17 e system: Electron-pair coupling between trigonal planar-like Ni(I) and tetrahedral-like Ni(I). [d] 15 e−15 e system: Electron-pair coupling between two trigonal planar-like Ni(I) atoms. [f] This study.

shorter than that between two tetrahedral-like Ni(I) in each 34-electron dimer. Particularly noteworthy is that this observed general trend of a shorter Ni−Ni′ bond length in each 32-electron $Ni_2(\mu_2\text{-}PR_2)_2$ dimer relative to that in each 34-electron $Ni_2(\mu_2\text{-}PR_2)_2$ dimer may also arise from significant multiple-bond character in the 32-electron dimer, which from a formal valence electron count conforms to a Ni−Ni′ double bond. Similarly, the analogous trend of a shorter Ni−Ni bond length in each 30-electron $Ni_2(\mu_2\text{-}PR_2)_2$ dimer versus that in a 32-electron $Ni_2(\mu_2\text{-}PR_2)_2$ dimer may likewise reflect greater multiple-bond character of the Ni−Ni′ bond in the 30-electron dimer.

The observations from Table 4 that the 34-electron $Ni_2(PMe_3)_4(\mu_2\text{-}P(H^tBu)_2)_2$[47] has a 0.05 Å-longer Ni−Ni′ bond length than that in the two 34-electron $Ni_2(CO)_4(\mu_2\text{-}PR_2)_2$ (R = Ph,[44] ^{t}Bu[45]) and that the 32-electron $Ni_2(CO)_2(PMe_3)(\mu_2\text{-}P^tBu_2)_2$[47] similarly has a 0.04 Å-longer Ni−Ni′ bond length than that in the 32-electron $Ni_2(CO)_3(\mu_2\text{-}P^tBu_2)_2$[47] are both consistent with the premise that the replacement of a π-acceptor CO ligand with a much better σ-donor PMe_3 ligand would significantly increase the negative charge density on each Ni(I) and thereby would result in a longer Ni−Ni′ bond length. Hence, it is apparent that the nature of the terminal L ligands (*i.e.*, both electronic/steric effects) can also influence Ni−Ni′ bond lengths. Nevertheless, even in the absence of detailed MO calculations from which one could possibly correlate net Ni−Ni′ overlap populations in these dimers with their Ni−Ni′ bond lengths, the observed structural/bonding trends outlined above provide a self-consistent basis for our belief that the Ni−Ni′ bonding interactions in these 34-, 32-, and 30-electron $Ni_2(\mu_2\text{-}ER_2)_2$ dimers (E = P, As, Sb) play a dominant role in controlling the similarly sharp angular deformations of the Ni_2E_2 rings and hence the stabilities of the dimers.

The resulting 0.25 Å-longer electron pair Ni−Ni′ bond in the Ni_2E_2 rhombus of the 34-electron $Ni_2(CO)_4(\mu_2\text{-}E\text{-}^tBu_2)_2$ when E is changed from P to Sb emphasizes that metal−metal distances in ligand-bridged dimers do not generally give a valid estimate of either metal radii of metal−metal bond orders.

The structural feature common to the 11 Ni−Ni′-bonded $Ni_2(\mu_2\text{-}ER_2)_2$ dimers (E = P, As, Sb) found in Table 4 is the presence of bulky E-attached R substituents which apparently provide steric protection of the two electron-pair coupled Ni(I) from air oxidation. It is clear that the essential ingredient in the design of other stable analogues lies in the use of analogous highly hindering R substituents. In a similar fashion, West and co-workers[68] have shown that the key to the syntheses of stable disilenes involves protection of the Si−Si double bond from air oxidation by sterically hindering substituents, which in general also cause a decrease in disilene reactivities as the size of the substituents increases.

Over 25 years ago we proposed[69] that formation of the electron-pair metal−metal bond is the controlling influence for the solid-state dimerization of $Fe(NO)_2I$ to give the analogous isostructural 34-electron $Fe_2(NO)_4(\mu_2\text{-}I)_2$, as opposed to the possible alternative polymeric structure of $Co(NO)_2I$ which in the solid state consists of infinite parallel chains formed by equally oriented tetrahedral-like $Co(NO)_2I_2$ units sharing the common corners of both iodine atoms. At that time we analyzed the influential role of the particular coordination about each metal atom in dictating the kind of angular deformation of the M_2E_2 ring from a metal−metal interaction as illustrated for five-, six-, and seven-coordinated metal atoms. It was then shown that ligand-bridged complexes containing a known metal−metal electron pair bond can generally be distinguished from those without metal−metal interactions by their significantly more acute bridging angles.

Experimental Section

Methods and Materials. All reactions including sample transfers and manipulations were carried out with standard Schlenk techniques either on a preparative vacuum line under

(68) (a) Shepherd, B. D.; Powell, D. R.; West, R. *Organometallics* **1989**, *8*, 2664−2669. (b) West, R. *Angew. Chem., Int. Ed. Engl.* **1987**, *26*, 1201−1211. (c) Okazaki, R.; West, R. *Adv. Organomet. Chem.* **1996**, *39*, 231−273.

(69) Dahl, L. F.; Rodulfo de Gil, E.; Feltham, R. D. *J. Am. Chem. Soc.* **1969**, *91*, 1653−1664.

nitrogen or within a Vacuum Atmospheres drybox under nitrogen atmosphere. The following solvents were freshly distilled under nitrogen from the indicated appropriate drying agents immediately prior to use: hexane (CaH_2); toluene (Na/benzophenone); tetrahydrofuran (K/benzophenone); acetone ($CaSO_4$); acetonitrile (Na_2CO_3); diisopropyl ether (K/benzophenone); diethyl ether ($CaCl_2$).

The $[NMe_4]^+$ salt of the $[Ni_6(CO)_{12}]^{2-}$ dianion (**1**) was prepared by a modification of the general method of Longoni, Chini, and Cavalieri.[39,70] The following materials were used without further purification: magnesium metal turnings (Fisher), carbon tetrachloride (Mallinckrodt), antimony trichloride (Aldrich), iodomethane (Aldrich), bromine (Mallinckrodt), iodoethane (Aldrich), 2-bromopropane (Aldrich), 2-bromo-2-methylpropane (Aldrich), 1,2-dibromoethane (Aldrich). Silica (Kieselgel 60, 230−400 mesh; Merck) was activated by being heated to 150 °C for 48 h under vacuum; distilled water (7% by weight) was then added to the cooled silica under nitrogen to ensure a consistent activity.

Infrared spectra were obtained on either a Mattson Polaris FT-IR or a Nicolet 740 FT-IR spectrophotometer. Solution spectra were obtained by use of nitrogen-purged CaF_2 cells. The carbonyl frequencies reported were observed in the 1600−2200 cm^{-1} window; peaks due to solvents, water, and decomposition products such as $Ni(CO)_4$ are not reported.

Preparations of Alkylantinomy Halides.[71] **(a) Dimethylantimony Bromide.** The preparation of the trimethylantimony dibromide, an intermediate obtained at 74% yield, was carried out on a 20% scale of that published previously.[72] The synthesized, white, air-stable Me_3SbBr_2 was heated in a small Schlenk flask equipped with a reflux condenser that was attached to a high-vacuum line; this procedure involving thermolysis and subsequent distillation at 200 °C and *ca.* 50 Torr afforded pure dimethylantimony bromide as a yellow oil. At lower temperatures thermolysis to the desired product did not occur; instead, only sublimed Me_3SbBr_2 was isolated. Because dimethylantimony bromide is highly reactive with oxygen and water and decomposes easily, this compound either was utilized as a reagent within short periods of time or was hermetically sealed in an ampule under vacuum.

(b) Diethylantimony Bromide. Although the intermediates obtained in synthesizing Et_2SbBr are analogous to those obtained in preparing Me_2SbBr, the reaction conditions were changed markedly to reflect the higher boiling point of triethylantimony (*viz.*, bp of 160 °C vs that of 79 °C for Me_3Sb). The synthesis was carried out in a similar fashion to that given elsewhere.[73] This dense, viscous oil did not seem to decompose as rapidly as that of the Me_2SbBr, if kept at −10 °C in hermetically sealed vials.

(c) Diisopropylantimony Bromide. Conditions similar to those for obtaining the ethyl analogue were used. $^iPr_2SbBr$ was isolated as a clear, yellow oil that seemed less viscous than the ethyl or methyl analogues; this compound was also be kept at −10 °C in sealed vials to prevent its decomposition.

(d) Di-*tert*-butylantimony Chloride. 1,2-Dibromoethane (6.0 mL, 13.1 g, 69 mmol) and 50 mL of diethyl ether were added to magnesium metal (18.0 g, 740 mmol) inside a three-neck 1.0 L flask equipped with a septum, a reflux condenser, a nitrogen/vacuum inlet, and a stirbar. After the evolution of ethylene ceased, 57.6 mL (68.5 g, 500 mmol) of *tert*-butyl bromide dissolved in 200 mL of diethyl ether was added at 13 °C over a period of 6 h. Refluxing for 20 min to ensure completion of reaction was followed by a transfer of the ether-soluble contents to a 1.0 L Schlenk flask containing a stirbar and 43.3 g (190 mmol) of antimony trichloride dissolved in 150 mL of diethyl ether at −25 °C. Addition of 300 mL of saturated ammonium chloride aqueous solution resulted in a gas evolution. The ether layer was evaporated in a nitrogen stream for 40 h, after which the residue was filtered to give 11.3 g (41.7 mmol, 22% yield) of di-*tert*-butylantimony chloride as a yellow oil. This product was used for subsequent work without further purification.

(e) $(p\text{-}FC_6H_4)_2SbCl$. Synthesis of the tris(*p*-fluorophenyl)-antimony intermediate was carried out (75% yield) in a similar manner as described in the literature;[74] this compound was reacted further[56] to give the desired $(p\text{-}FC_6H_4)_2SbCl$, in essentially 100% yield.

The identity of $(p\text{-}FC_6H_4)_2SbCl$ was established from a mass spectrum (Kratos MS-25 spectrometer; electron-impact ionization). The sample was introduced into the ion source via a heated probe. The ion-fragment pattern observed in the positive-ion mass spectrum includes the following: ion-parent peak at $m/z = 347.95$ ($[M]^+$, 7%), 345.95 ($[M]^+$, 7%); ion peaks at 310.96 ($[(p\text{-}FC_6H_4)_2Sb]^+$, 28%), 308.96 ($[(p\text{-}FC_6H_4)_2Sb]^+$, 18%), 252.90 ($[(C_6H_4F)SbCl]^+$, 16%), 250.91 ($[(C_6H_4F)SbCl]^+$, 17%); 217.93 ($[(C_6H_4F)Sb]^+$, 58%), 215.93 ($[(C_6H_4F)Sb]^+$, 68%), 190.06 ($[(C_6H_4F)_2]^+$, 100%); 157.88 ($[SbCl]^+$, 15%), 155.88 ($[SbCl]^+$, 17%); 95.03 ($[C_6H_4F]^+$, 13%).

Preparation of Icosahedral $[Ni_{10}(SbR)_2(CO)_{18}]^{2-}$ Clusters as $[NMe_4]^+$ Salts. (a) $[Ni_{10}(SbMe)_2(CO)_{18}]^{2-}$ Dianion (3). In a typical reaction 0.44 g (2.0 mmol) of freshly prepared dimethylantimony bromide dissolved in 20 mL of THF was slowly dripped into a stirred solution containing 0.84 g (1.0 mmol) of $[NMe_4]_2[Ni_6(CO)_{12}]$ dissolved in 80 mL of THF in a 250 mL Schlenk flask. The solution turned from a red to brown color. An IR spectrum taken 2 h later showed no carbonyl bands characteristic of $[Ni_6(CO)_{12}]^{2-}$; the reaction mixture was then filtered from an insoluble residue, and the solvent was evaporated under a nitrogen stream. The residue was a mixture of white and black powders (presumably NMe_4Br and an insoluble nickel bromide compound that produced a green powder upon exposure to air). Hexane extractions of the THF fraction were colorless. Toluene extractions yielded about 35 mg of an unidentified air-sensitive, dark brown solid upon evaporation of the solvent. THF extracts resulted in a dark brown solution which upon evaporation gave 364 mg of dark brown solid. This solid was recrystallized from a concentrated THF solution via a layering of either isopropyl ether or hexane over the THF and, alternatively, via the slow removal of the THF solvent under a nitrogen stream. An X-ray diffraction investigation of these crystals established them to be $[NMe_4]_2[Ni_{10}(SbMe)_2(CO)_{18}]$. An IR spectrum (THF) of crystals of this compound revealed carbonyl bands at 2004 (s) and 1834 (m) cm^{-1}.

(b) $[Ni_{10}(SbEt)_2(CO)_{18}]^{2-}$ Dianion (4). The preparation of this compound followed a similar procedure utilized for obtaining the methyl analog. A sample (1.2 g, 4.6 mmol) of diethylantimony bromide dissolved in 20 mL of CH_3CN was slowly added to 1.9 g (2.3 mmol) of $[NMe_4]_2[Ni_6(CO)_{12}]$ dissolved in 30 mL of CH_3CN. The solution color turned from red to brown; the soluble material was filtered and evaporated under a nitrogen stream. Unlike that for the methyl analogue, extractions with hexane dissolved about 5−10% by weight of the residue. An IR spectrum (hexane) of the hexane extract exhibited carbonyl maxima at 2068 (w, sharp), 1997 (s, sharp), and 1961 (w) cm^{-1}. The majority of the remaining residue was soluble in toluene. Crystallization of this unstable extract was not successful; an IR spectrum (THF) revealed maxima at 1990 (s), 1953 (w), and 1891 (w) cm^{-1}. The residue remaining in the reaction flask was then extracted with THF and crystallized in a similar manner to that of the methyl analogue. An

(70) Ceriotti, A.; Longoni, G.; Piva, G. *Inorg. Synth.* **1989**, *26*, 312−315.

(71) It should be noted that distillation, refluxing, or other experimental manipulations in the synthesis of this and related antimony monomeric compounds need to be carried out in a tightly sealed apparatus under a hood with closed sashes; leakage from apparatus during the distillation of trimethylantimony, even in a well-working hood, may give rise to metal poisoning-like symptoms—*viz.*, vertigo, myopia, peripheral neuropathy, and/or vomiting.

(72) Doak, G. O.; Long, G. G.; Key, M. E. *Inorg. Synth.* **1967**, *9*, 92−97.

(73) Issleib, K.; Hamann, B. *Z. Anorg. Allg. Chem.* **1965**, *339*, 289−297.

(74) de Ketelaere, R. F.; Delbeke, F. T.; van der Kelen, G. P. *J. Organomet. Chem.* **1971**, *30*, 365−368.

IR spectrum (THF) of crystals of **4** as the $[NMe_4]^+$ salt displayed bands at 2007 (s), 1967 (sh), and 1829 (m) cm^{-1}. If the above reaction is carried out under the same conditions in THF solution (instead of acetonitrile), all extracts yield residues in similar amounts with similar IR spectra.

(c) $[Ni_{10}(Sb^iPr)_2(CO)_{18}]^{2-}$ Dianion (5). The synthesis of this compound is similar to those outlined above. A sample (1.0 g, 3.5 mmol) of diisopropylantimony bromide dissolved in 30 mL of THF was slowly dropped into a stirred solution of $[NMe_4]_2[Ni_6(CO)_{12}]$ (1.5 g, 1.7 mmol) suspended in 30 mL of THF. The THF-soluble products were separated from the small quantity of residue by filtration; the THF was removed under a nitrogen stream and the residue sequentially extracted with hexane, toluene, and THF. Evaporation of the brown hexane extract gave an unstable oily residue; an IR spectrum (THF) indicated a mixture of compounds with bands at 2076 (w), 2057 (s), 2047 (m), 2021 (s), 2000 (s), 1984 (m), 1965 (s), 1860 (w), and 1812 (w) cm^{-1}. The THF extract gave a brown solid upon evaporation of the solvent; crystallization from a concentrated THF solution layered with hexane produced **5** as the $[NMe_4]^+$ salt. An IR spectrum (THF) exhibited bands at 2006 (s), 1970 (sh), and 1825 (m) cm^{-1}. An identical IR spectrum (THF) obtained from the toluene extract showed that the compound is markedly soluble in toluene as well as in THF.

(d) $[Ni_{10}(Sb^tBu)_2(CO)_{18}]^{2-}$ Dianion (6). Di-*tert*-butylantimony chloride (1.8 g, 6.6 mmol) dissolved in 20 mL of THF was slowly added at room temperature to $[NMe_4]_2[Ni_6(CO)_{12}]$ (2.5 g, 3.0 mmol) suspended in 50 mL of THF. After 150 min the reaction mixture was extracted from the THF-insoluble products. The residue left in the reaction flask contained a mixture of an acetone-soluble compound (IR spectrum (MeCN): 1999 (s), 1840 (m), and 1805 (sh) cm^{-1}), an acetonitrile-soluble compound (IR spectrum (MeCN): 1993 (s) cm^{-1}), and a grayish-green powder presumed to be $NiCl_2$. The solvent from the THF extract was evaporated and the residue sequentially extracted by hexane, toluene, and THF. The hexane extract was a mixture of products, while the toluene extract (IR spectrum (THF): 1979 (s) and 1832 (m) cm^{-1}) readily decomposed to a beige, toluene-insoluble powder. The brown THF-soluble residue was crystallized from a concentrated solution of THF layered with hexane to give **6** as the $[NMe_4]^+$ salt. An IR spectrum (THF) of this compound revealed carbonyl bands at 2007 (s), 1975 (sh), 1817 (m), and 1785 (br) cm^{-1}.

(e) $[Ni_{10}(Sb(p\text{-}FC_6H_4))_2(CO)_{18}]^{2-}$ Dianion (7). The preparation of this compound was performed in a similar manner as that of the phenylantimony analogue (**2**).[29] A sample (1.0 g, 2.9 mmol) of bis(*p*-fluorophenyl)antimony chloride dissolved in 30 mL of acetone was added slowly to 50 mL of acetone containing 1.2 g (1.4 mmol) of $[NMe_4]_2[Ni_6(CO)_{12}]$. After being stirred for 3 h, the solvent was evaporated under a nitrogen stream. Extraction of the isolated residue with hexane gave no soluble material. Only a little material, which readily decomposed, was isolated from the toluene-soluble extract; an IR spectrum (THF) showed bands at 2019 (s), 2003 (m), 1960 (s), and 1928 (sh) cm^{-1}. The remaining residue dissolved with some difficulty in THF; an IR spectrum indicated a mixture of products. Hence, the THF extract was loaded onto a silica column and chromatographed (eluent: 50% THF, 50% acetone by volume); the second band gave a brown solid which, upon evaporation of the eluent, was identified as the $[NMe_4]^+$ salt of **7**. An IR spectrum (THF) displayed bands at 2017 (s), 2000 (sh), and 1831 (m) cm^{-1}.

(f) $[Ni(CO)_2Sb^tBu_2]_2$ (8). Di-*tert*-butylantimony chloride (1.8 g, 6.6 mmol) dissolved in 20 mL of THF was slowly added at room temperature to $[NMe_4]_2[Ni_6(CO)_{12}]$ (2.5 g, 3.0 mmol) dissolved in 50 mL of THF. After 150 min the reaction mixture was extracted from THF-insoluble products. The hexane extract of the residue obtained after evaporation of the THF solvent was separated via column chromatography. The first dark yellow band off the column gave yellow-brown block crystals upon evaporation of the solvent into either decahydronaphthalene or toluene.

(g) Synthesis and Reaction of Phenylmethylantimony Halide with $[NMe_4]_2[Ni_6(CO)_{12}]$. The synthesis of the phenylantimony dibromide intermediate was carried out in a similar manner as outlined elsewhere.[56] Solid triphenylantimony (17.7 g, 50 mmol) was added to solid antimony tribromide (36.2 g, 100 mmol). These two powders liquefy upon contact to form a yellowish oily liquid. Heating the mixture to 80 °C to ensure completion of reaction gave phenylantimony dibromide, which was used without further purification.

Magnesium turnings (3.4 g, 140 mmol) and 100 mL of diethyl ether were added to a 3-neck 500 mL flask equipped with a nitrogen/vacuum inlet, a reflux condenser, and a stirbar. Iodomethane (8.7 mL, 19.9 g, 140 mmol) mixed with 200 mL of diethyl ether was slowly dripped into the flask via 20-gauge steel hypodermic tubing. The resulting methylmagnesium iodide was then added dropwise to phenylantimony dibromide to obtain only partial methylation of the antimony reagent; it is important not to do this addition in reverse order in order to prevent the formation of a mixture of phenyldimethylantimony and unreacted phenylantimony dibromide and further metathesized products thereof. After being stirred for 2 h, the solvent was evaporated by a nitrogen stream, and the remaining oil sublimed under high vacuum to give 3.0 g of a highly air-sensitive crystalline solid. Comparison of the mass spectrum peaks (Kratos MS-80 spectrometer; electron-impact mode) of this solid with those reported[75] for PhMeSbBr and PhMeSbI revealed it to be a mixture of phenylmethylantimony bromide and phenylmethylantimony iodide. The THF extract of the solid resulting from reaction of this PhMeSbBr/PhMeSbI mixture with the $[NMe_4]^+$ salt of the $[Ni_6(CO)_{12}]^{2-}$ dianion (**1**), carried out under similar conditions as those utilized for obtaining the other Ni−Sb icosahedral clusters, provided crystals of $[NMe_4]_2[Ni_{10}(SbMe)_2(CO)_{18}]$; the identity of this compound was ascertained from a single-crystal X-ray diffraction study, which showed that the unit cell parameters compared favorably with those previously determined for the methylantimony compound. No nickel−antimony carbonyl clusters with phenyl substituents (such as **2**) were isolated from this reaction.

Characterization of $[Ni_{10}(SbR)_2(CO)_{18}]^{2-}$ (R = Me (3), Et (4), ^{i}Pr (5), ^{t}Bu (6), *p*-FC_6H_4 (7)). These air-sensitive, dark brown compounds were prepared as $[NMe_4]^+$ salts. Crystals of $[NMe_4]_2$[**3**] decompose in a nitrogen atmosphere to a black powder at 207−209 °C (uncorrected, determined on the Unimelt capillary melting point apparatus). The stoichiometry of this compound established by the structural determination was ascertained from an elemental analysis (Desert Analytics, Tucson, AZ) of a recrystallized sample of $[NMe_4]_2$-[**3**]. Anal. Calcd for $C_{28}H_{30}N_2Ni_{10}O_{18}Sb_2$: C, 22.23; H, 2.00; N, 1.85; Ni, 38.79; Sb, 16.09. Found: C, 22.46; H, 1.98; N,1.68; Ni, 38.58; Sb, 16.10.

Electrochemical measurements were performed with a Bioanalytical Systems Electrochemical Analyzer in concert with a Princeton Applied Research electrochemical cell operating inside of a Vacuum Atmosphere drybox. The cell consisted of a glassy carbon working electrode, a platinum wire auxiliary electrode, and a standard calomel electrode (SCE). All voltage potentials were measured relative to the SCE; the reversible ferrocene/ferrocenium cation system was used as an internal standard for selected compounds. The voltammogram was recorded at scan rates of 20, 50, 100, and 500 mV/s. Recrystallized samples of $[NMe_4]_2$[**3**] and $[NMe_4]_2$[**5**] displayed an irreversible oxidation at ca. +0.60 V in acetonitrile solutions.

A negative-ion ESI mass spectrum of $[NMe_4]_2$[**5**] was performed with a VG-AutoSpecE mass spectrometer (mass range 200−4000; electrospray ionization; 2000 resolution; time, 4.00 s/dec; delay, 0.50 s; accelerating voltage, 4000.0 eV). The following high-range m/z signals with assigned doubly charged ion-fragment formulas were observed: m/z 710.0 ($[M]^{2-}$, 0.7%); 696.0 ($[M - CO]^{2-}$, 0.5%); 682.0 ($[M - 2CO]^{2-}$, 1.1%); 668.0

(75) Henrick, K.; Mickiewicz, M.; Roberts, N.; Shewchuk, E.; Wild, S. B. *Aust. J. Chem.* **1975**, *28*, 1473−1488.

([M − 3CO]$^{2-}$, 1.3%); 653.9 ([M − 4CO]$^{2-}$, 1.8%); 632.0 ([M − 4CO − C_3H_7]$^{2-}$, 6.8%); 625.0 ([M − 3CO − 2C_3H_7]$^{2-}$, 1.0%); 610.9 ([M − 4CO − 2C_3H_7]$^{2-}$, 59.5%); 597.0 ([M − 5CO − 2C_3H_7]$^{2-}$, 100.0%); 583.0 ([M − 6CO − 2 C_3H_7]$^{2-}$, 23.8%); 568.9 ([M − 7CO − 2C_3H_7]$^{2-}$, 2.1%); 554.9 ([M − 8CO − 2C_3H_7]$^{2-}$, 0.4%). A complex isotopic pattern was obtained for each signal due to nickel having five naturally occurring isotopes (*viz.*, ^{58}Ni, 68.1%; ^{60}Ni, 26.2%; ^{61}Ni, 1.1%; ^{62}Ni, 3.6%; ^{64}Ni, 0.9%) and antimony having two naturally occurring ones (*viz.*, ^{121}Sb, 57.4%; ^{123}Sb, 42.6%). Each complex isotopic pattern provided a basis for determining unambiguously the assigned formula by a matching of the resulting calculated isotopic pattern with the observed one. For example, the strongest signal centered at *m*/*z* 597 has an observed isotopic pattern consisting of approximately 24 peaks, of which the 11 central peaks have relative values of 53:13:84:23:100:27:90:23:72:23:47 versus calculated ones[62] of 53:11:85:20:100:27:91:25:68:19:43 for the assigned formula of [$Ni_{10}Sb_2(CO)_{13}$]$^{2-}$ (denoted as [M − 5CO − 2C_3H_7]$^{2-}$). In addition, there were a number of smaller peaks in the *m*/*z* 200−400 range that were likewise assigned to ion-fragments containing one to four nickel and antimony atoms.

A solid-state magnetic susceptibility measurement at room temperature via a TME balance conclusively showed a powder sample of [NMe_4]$_2$[**3**] to be diamagnetic.

A ^{1}H NMR spectrum (250 MHz, acetone-d_6 at 23 °C) of recrystallized [NMe_4]$_2$[**3**] exhibited the following: δ 1.93 ($SbCH_3$, 6H, s) and 3.45 ppm ($N(CH_3)_4^+$, 24H, s). The observed chemical shift of the methylantimony proton peak corresponds within 0.4 ppm to those of methylantimony proton peaks in antimony-trimetalated Sb−CH_3 organometallic clusters.[76] A ^{13}C{^{1}H} NMR spectrum (126 MHz, acetone-d_6 at 213 K) of [NMe_4]$_2$[**3**] displayed signals at δ −4.16 ($SbCH_3$), 54.04 ($N(CH_3)_4^+$), 191.77 (*C*O(terminal)) and 240.82 ppm (*C*O(bridging)).

A ^{13}C{^{1}H} NMR spectrum (125.7 MHz, acetone-d_6 at 213 K) of [NMe_4]$_2$[**5**] exhibited resonances (referenced to the 206.0 ppm acetone peak) at δ 23.9 ((CH_3)$_2$CH−), 25.8 ((CH_3)$_2$*C*H−), 54.0 ($N(CH_3)_4^+$), 193.5 (*C*O(terminal)), and 242.1 ppm (*C*O(bridging)). At room temperature the carbonyl peaks were not observed due to extensive broadening.

Variable-temperature measurements of [NMe_4]$_2$[**5**] were taken at 10 K intervals from 213 to 293 K. About 0.6 mL of vapor-diffused and triply degassed acetone-d_6 was saturated with [NMe_4]$_2$[**5**] and then diluted to 1.0 mL in a 5 mm NMR tube, which was then flame-sealed under vacuum. For the variable-temperature ^{13}C{^{1}H} NMR investigation the following variables were used: a Brucker AM-500 instrument was operated at 125.7 MHz synthesizer frequency, at pulse widths of 5.0 μs, for several thousand pulses at each temperature (temperatures were measured by a standard technique;[77] ±0.5 K relative error). The precise peak widths, which were used in the DNMR calculation, were measured from spectra scanned only in 500 Hz sweep-width windows.

X-ray Crystallographic Determinations and Refinements. Each crystal was mounted under an argon atmosphere onto a thin glass fiber and coated with epoxy inside a Lindemann glass capillary which was then hermetically sealed. Intensity data were obtained with graphite-monochromated Mo Kα radiation on refurbished Siemens P$\bar{1}$, Siemens P3/F, or Siemens P4 diffractometers equipped with either a Mo sealed tube generator or a rotating Mo anode generator. Unit-cell determinations were based upon well-centered reflections; axial photographs were taken to verify lattice lengths. For each structural determination the intensities of standard reflections showed no significant variations during the entire collection of data. Empirical absorption corrections based upon ψ-scans measurements at different azimuthal angles were applied to each data set. Crystallographic computations were carried out either with SHELXTL PLUS or SHELXTL 93 run either on a VAX computer or a Silicon Graphics Indy workstation. Initial positions for the heavy atoms were found by direct methods, and positions of the light non-hydrogen atoms were determined from successive Fourier difference maps coupled with preliminary isotropic least-squares refinement. The refinement method was full-matrix least squares on the F^2. All non-hydrogen atoms were subsequently refined anisotropically; the hydrogen atoms were placed at idealized positions with fixed isotropic thermal parameters and refined by use of a riding model. A final Fourier difference map showed no unusual features for each structure.

Crystal data, data-collection, and refinement parameters for the [NMe_4]$^+$ salts of **3**−**7** and for the neutral dimeric **8** are given in Table 1. Configurations[57,58] of the entire dianions, **3**−**7**, are shown in Figures 1a and 2a−d, respectively. The space-filling models of **3** and **6** are compared in Figure 3, and the 1,12-$Ni_{10}Sb_2$ icosahedral cage of **3**, typical of these dimers, is shown in Figure 1c.

Acknowledgment. We greatly appreciate the financial support of this research by the National Science Foundation (Grants CHE-9013059, CHE-9310428). Departmental purchase of the X-ray diffractometers and associated computer equipment utilized in this work was made possible by funds from the NSF (Grant CHE-9105497) and the Graduate School of UW−Madison. We are particularly indebted to Dr. Randy K. Hayashi and Dr. John Bemis (Chem. Dept., UW−Madison) for their X-ray crystallographic assistance. We are also very grateful to Professor Charles P. Gibson (Chem. Dept., UW−Oshkosh) for the magnetic susceptibility measurements, to Dr. Marcel Hop (Chem. Dept., UW−Madison) for the ESI mass spectrometric measurements, and to David Snyder (Chem. Dept., UW−Madison) for the EI mass spectrometric measurements.

Supporting Information Available: Crystallographic tables for the [NMe_4]$^+$ salts of [$Ni_{10}(SbMe)_2(CO)_{18}$]$^{2-}$ (**3**), [$Ni_{10}(SbEt)_2(CO)_{18}$]$^{2-}$ (**4**), [$Ni_{10}(Sb^iPr)_2(CO)_{18}$]$^{2-}$ (**5**), [$Ni_{10}(Sb^tBu)_2(CO)_{18}$]$^{2-}$(**6**), and [$Ni_{10}(Sb(p\text{-}FC_6H_4))_2(CO)_{18}$]$^{2-}$ (**7**) and for the neutral [$Ni(CO)_2(\mu_2\text{-}Sb^tBu_2)$]$_2$ (**8**), including atomic coordinates, anisotropic thermal displacement parameters, interatomic distances, bond angles, and idealized hydrogen coordinates (35 pages). Ordering information is given on any current masthead page.

OM960966C

(76) Malisch, W.; Panster, P. *Chem. Ber.* **1975**, *108*, 716−723.
(77) Sandstrom, J. *Dynamic NMR Spectroscopy;* Academic Press: London, U.K., 1982; pp 71−76.